THE EFFECT OF BALL MILL OPERATING PARAMETERS ON MINERAL LIBERATION

by

Hector E. Rojas

Dissertation submitted to the Faculty of the
Virginia Polytechnic Institute and State University
in partial fulfillment of the requirements for the degree of

Masters of Science

in

Mining and Minerals Engineering

APPROVED:

G. T. Adel, Chairman

R. H. Yoon

G. H. Luttrell

M. E. Karmis

November, 1989

Blacksburg, Virginia

THE EFFECT OF BALL MILL PARAMETERS ON MINERAL LIBERATION

by

Hector E. Rojas

Committee Chairman: Dr. G.T. Adel
Mining and Mineral Engineering

(ABSTRACT)

In previous studies, the analysis of ball mill operating parameters and their effects on breakage phenomena has been limited to homogeneous materials. Though these studies have proven to be an asset in predictions of product size distributions and mill scale-up, they have not addressed the primary role of grinding, i.e. liberation.

The present investigation analyzes the effect of ball mill operating parameters on the breakage rates of both liberated and composite material. The operating parameters studied include mill rotational speed, ball size, mill charge and wet versus dry grinding. Breakage rates have been determined experimentally utilizing a SEM-IPS image analyzer. The mineral sample used was acquired from ASARCO's Young Mine which is located in Jefferson City Tennessee. It was a binary ore consisting of sphalerite and dolomite.

Batch grinding experiments were conducted to provide breakage rates for the various composition classes. Breakage rates were then normalized with respect to energy to see if the changes in breakage rates associated with mill operating parameters were due to changes in breakage kinetics, or simply a function of energy input.

The energy normalized data indicates that the free dolomite breakage rates tend to normalize with respect to energy in the case of varying interstitial fillings. Furthermore, changes in mill rotational speed tend to provide energy normalizable breakage rates for both free dolomite and sphalerite. In all other cases, analysis of the breakage rates and energy specific breakage rates indicate that a change in breakage kinetics may be occurring.

In general, particles containing a high proportion of sphalerite are more apt to break under impact conditions. On the other hand, particles containing a large proportion of dolomite were found to prefer attrition breakage conditions.

ACKNOWLEDGEMENT

The author wishes to express his appreciation for the support and encouragement provided by his advisor, Dr. G. T. Adel as well as the rest of the faculty at Virginia Tech. Their interest and involvement with this project made the time and effort a worthwhile experience. Special thanks are due to ASARCO for continuing its cooperation with Virginia Tech in providing mineral ore samples from its Young Mine operation.

This research has been supported by the Department of the Interior's Mineral Institute program administered by the Bureau of Mines through the Generic Mineral Technology Center for Comminution under grant # G1125149. The author wishes to extend his appreciation for this support as well as that provided by Dr. M. E. Karmis and the Department of Mining and Minerals Engineering for providing the author with tuition scholarships.

Recognition should be given to Roy Hill for performing the chemical assays as well as technical assistance with the scanning electron microscope. Special thanks are extended to Bloice Davison, Brian Robinette and Hillary Smith for their

help in sample preparation and polishing. Sincere gratitude is also extended to the numerous friendships that have been nurtured throughout the years at Virginia Tech with fellow graduate students, in particular those of Woo Zin Choi, Richard Forrest, Margie Lagno, Van Davis, Jennifer Smith, Michael Stallard, Joseph Zachwieja and Jorge Yordan.

The author wishes to express special acknowledgement to the loving support of his parents
Their encouragement and devotion made it all possible. As a third generation Mining Engineer, the author wishes to dedicate this thesis to his grandfather
whose exemplary career influenced the choice of this profession.

TABLE OF CONTENTS

LIST OF FIGURES

LIST OF TABLES

CHAPTER I

INTRODUCTION

1.1 Statement of Problem

Comminution is the process of physically breaking run-of-mine ore in order to achieve the liberation of valuable minerals from gangue. The process itself is very energy intensive and it is estimated that nearly two percent of the United States power consumption is related to comminution (Comminution and Energy Consumption, 1981). With this in mind it is understandable that one would want to control a grinding circuit so that the energy required to process a given ton of ore is optimal. Furthermore, overgrinding an ore and the subsequent production of fines can reduce the efficiency of later stages in the circuit such as flotation.

In order to study the behavior of grinding circuits, several attempts have been made to describe power consumption and its relation to size reduction. Three theories that have been used to date are those of Rittinger (1867), Kick (1885), and Bond (1952). These approaches are limited in that they provide little or no information on expected size distributions. Furthermore, each approach is limited in its applicability to select particle size ranges.

A more practical approach to the understanding of the breakage phenomena is that of population balance modeling. By utilizing breakage rates and distribution functions, accurate predictions of product size distributions can be obtained for homogeneous materials. The advantage of this method as compared to the prior energy relationships, is its ability to allow simulation of grinding operations and predictions of product sizes under different mill conditions. Unfortunately, the present application of the population balance approach does not address the primary objective of grinding which is liberation.

With the onset of image analysis technology, liberation itself can now be quantified. This has lead to the evolution of grinding models which incorporate liberation as a parameter (Andrews and Mika; 1976, Peterson and Herbst; 1985, Choi 1986).

With the existing size reduction models, much work has been done in studying the effect of operating parameters such as mill speed and ball loading on model parameters and the resulting product fineness (Fossberg and Zhai; 1986, Herbst and Fuerstenau 1972; Houiller and Neste and Marchand 1976). It should be noted, however, that in each of these studies homogeneous material was used for the grinding experiments, thereby not including liberation as part of the study.

Although models for liberation have been developed, the effect of milling conditions on the liberation parameters of these models has not been evaluated. The purpose of this investigation is to determine if liberation can be changed by mill operating parameters. It is hoped that this work can be used as a precursor to the development of a model that can predict liberation given the various ranges of operating parameters. Mill speed, mill charge, ball size, and wet grinding are the parameters which have been selected for the present study. It is hoped that the analysis of the data acquired will allow insight as to which parameters will require a functional form if they were to be integrated into a complete liberation model.

1.2 Literature Review

1.2.1 Grinding Theories and Models

a. Grinding theories: The first attempt to relate size reduction to energy consumption was that of Rittinger (1867) who postulated that the energy consumption for size reduction is proportional to the area of the new surface produced. Later, Kick (1885) proposed that the energy required for size reduction is proportional to the reduction in the volume of the particles in question. The most widely used relation of this type however, was that of Bond (1952) who proposed that energy consumption is proportional to the

new crack tip length produced during breakage. Bond developed the well known Bond work index which is an indicator of a materials resistance to crushing and grinding. Each of these theories was useful in the design and scale up of ball mill operations, however they told little of the expected size distributions, and most importantly gave no indication of liberation.

Later work done by Hukki (1975) attempted to show the validity of each theory within a certain particle size range. This study illustrated that Kicks law was applicable in the crushing range (above 1 cm in diameter). Bond's theory was more suited to the particle size ranges involved in conventional ball and rod mill grinding (5 to 250 mm). Rittinger's law showed more applicability to the fine particle grinding range (10-1000 micro meters).

The development of mathematical models for size reduction began nearly 20 years ago. Unlike the theories that were based on the energy requirements, these models allowed the prediction of product size distributions based on experimentally determined constants. Their application was also well suited to simulations of grinding operations which greatly facilitated optimization studies on industrial scales.

An early attempt to describe the breakage process was that of Epstein (1947). His model utilized two basic

functions, the selection function [$S_n(y)$], which represents the probability of breakage of a particle in size class y, in the nth stage of breakage, and the distribution function, [B(x,y)], which represents the cumulative weight distribution of particles appearing below the size class x resulting from breakage out of a given size class y. His major assumption was that a particle would break into two smaller particles of the same size. Though this assumption was not realistic, it was this model that set the basis for further developments.

Modifying Epstein's scheme, Broadbent and Callcott (1956) developed a model which employed matrix operations to describe the breakage process. Size distributions were represented in terms of vector quantities which were determined from sieve evaluation. The assumption was made that the distribution function was not dependent on the grinding system, material, or the sizes considered and therefore remained constant. Though this matrix approach was unique and helpful in further models, it was limited by the fact that it's distribution function remained constant.

Using the matrix approach, Gardner and Austin (1962) modified the selection and distribution functions to incorporate a size-mass balance equation which contained a mass term in differential form with respect to time for each size class. In this modification, the selection function S_i

now represented the fractional rate at which the mass of a size class i was removed. They postulated that if one could determine the selection and distribution functions experimentally, that the size-mass balance equations could be solved for any feed sizes. A radio active tracer was used to determine breakage functions.

Much work has been done by various researchers to solve the grinding equations for product size distributions with relation to time (Herbst and Fuerstenau, 1968; Klimpel and Austin, 1970). Once the grinding equations were validated, work followed in scale up procedures for the design of continuous ball mill operations. (Herbst and Fuerstenau, 1980) The next section describes the mathematical basis for the discrete batch grinding model.

b. Population balance models: Analysis of grinding operations with regard to breakage rate, S, and breakage distribution function, B, has become a well established technique. Many researchers have worked in this area. (Austin, Bhatia 1971; Austin, Klimpel and Luckie, 1976; Gupta, Hodouin, Berube and Everell, 1981) These parameters allow the behavior of each size class in a mill to be described mathematically.

In the case of batch grinding, the general form for the size discretized relationship describing the rate of breakage from a given size class i is as follows:

$$dm_i(t) = \frac{b_{ij} * S_j * m_j(t)}{dt} - S_i * m_i(t) \qquad [1.1]$$

where $m_i(t)$ is the fraction of mass remaining at time t, b_{ij} is the fraction of material from size class j that reports to size class i after being reduced in size, S_j is the fractional rate at which the mass of the j-th size class is removed, and S_i is the fractional rate at which the mass of the i-th size class is removed. In general the breakage distribution term describes how material appears from upper size classes to a given size class. The breakage rate term describes how material disappears from a given size class. By grinding mono-sized material in dry batch tests, the breakage rate for that size material may be quantified. Since only mono-size material is present initially, the appearance term of Equation 1.1 drops out leaving the following relationship for a designated size class 1:

$$dm_1(t) = \frac{-S_1 m_1(t)}{dt} \qquad [1.2]$$

By first separating variables, and then integrating with respect to time from t=0 to t=t, equation [1.2] would be of the following form:

$$\ln(m_1(t)/m_1(0)) = - S_1*t \qquad [1.3]$$

S_1 can then be directly measured by plotting the natural log of the fraction remaining vs time. The resulting slope of this plot is S_1.

The determination of a cumulative breakage distribution function utilizes the concept of zero order production (the initial slope of the mass of fines being produced vs time). (Herbst and Fuerstenau, 1968) The following relation depicts the zero order rate constant in terms of its constituent values:

$$\frac{dY_i}{dt} = F_i \qquad [1.4]$$

where Y_i is the cumulative mass fraction finer than size class i and F_i is the zero order production constant for the production of material finer than size i ($time^{-1}$).

Various researchers have found that breakage rates remain constant with respect to time in the case of dry ball milling. (Herbst and Fuerstenau, 1968; Austin and Luckie 1971) This phenomenon allows the solution to the distribution function to be represented as follows:

$$B_{i1}*S_1 = F_i \qquad [1.5]$$

With the above relationships it is possible to solve for the model parameters which allow the prediction of product size distributions for homogeneous material. The next section describes the evolution of models which account for mineral liberation phenomenon as well as size reduction phenomena.

1.2.2 Liberation Theory and Models

a. Degree of liberation: The degree of liberation as described by Gaudin (1939) may be represented as follows for a particular mineral component:

$$L_i = 100 * \frac{W_i^f}{W_i^f + f_i W_i^l} \qquad [1.6]$$

where W_i^f is the number of the free mineral components i, W_i^l is the equivalent number of the locked mineral components, and f_i is defined as the locking factor which acts as a weighting factor to account for locked particles that may appear free during areal examination of a prepared mineral sample. Measurement of the degree of liberation gives insight as to the optimum grind for a given ore. This value may be used as a criterion to limit overgrinding and still achieve sufficient liberation to allow future stages in the processing circuit to be efficient. The development of image analysis techniques has made the determination of

the degree of liberation of a mineral component a simpler and less tedious task.

b. Liberation modeling: The first attempt aimed at modeling liberation was that of Gaudin's (1939). He proposed a model for the fracture of an ideal binary system composed of cubic components. From basic mathematical relationships the percentage of liberated material that could be expected was calculated. Furthermore, the concept of a degree of liberation was introduced. In order to quantify the degree of liberation, a microscope counting technique was described which allowed the estimation of a particles composition. The model itself however, was unrealistic since a cubic system was used along with cubical fracture patterns which resulted in cubical particles.

It was not until 1967 that Wiegel and Li attempted to modify Gaudin's model to allow a random orientation of mineral grains rather than placing grains of least abundant minerals as far apart as possible. A further modification allowed this model to account for different mineral content among composite materials. Though this model was indeed improved from its previous version, it still was limited by the cubic system assumption.

With the advent of computerized image processing systems in the late 1970's advances in the modeling of liberation followed. King (1979) developed a model which

was based on mineral grade distributions derived from linear grade intercepts. It was assumed that the ore was isotropic, and had no tendency to fracture preferentially along grain boundaries. Although this model was notably better in predicting liberation values than previous models, significant deviations from expected values were noted with particles greater than 400 microns. This could have been due to the assumptions that particles are isotropic and that random breakage is the primary breakage mechanism. Contrary evidence which indicates that preferential breakage is present has been established (Choi 1982).

Following Wiegel's model, an attempt to model the liberation of pyrite and ash from coal (Klimpel and Austin, 1983; Bagga and Luckie, 1983) utilized a Monte Carlo Simulation technique to randomly create particles with mineral grains. By making the computer generate specified size distributions, the amount of liberation could be evaluated for different grinds. In general, this model was developed for binary systems and was limited to random fractures only. It also required that the amount of one of the binary constituents be small in a composite particle (a common occurrence in many mineral systems). The model itself was validated with experimental data derived from a synthetic ore composed of polystyrene, pyrite, and quartz. The excellent agreement between the model predictions and

experimental data gave credence to the assumption that random fractures were dominant in this mineral system.

Recently an index to describe the degree of liberation was developed (Davy, 1984). The index varied from 0 to 1, the value of which was found to be related to the shape and size of the particles as well as to the interaction between fracture surfaces and the structure of the mineral. Using Davy's theory, a liberation model which utilized a random Poisson Polyhedra for fracture and fragment distributions from narrowly sized mono-sized particles was developed (Barbery, 1985).

Though much advancement in liberation modeling has occurred, the limiting factor of each model has been its constraint to open circuit simulation. Each of the models described assess the expected liberation that would occur, but do not address the relative abundance of each type of material composition. In the case of closed circuits, a classification mechanism such as a hydrocyclone is affected not only by particle size but mineral composition as well. For this reason, the introduction of varying amounts of composite and liberated material back into the circuits requires the knowledge of mass balances for each composition of particles.

Initial attempts at the modeling of both size reduction and liberation all encompassed limiting assumptions that

either made the model unrealistic with regard to physical breakage phenomena, or did not provide accurate predictions of liberation. Andrews and Mika (1975) modified the population balance model for grinding to incorporate a description of mineral particles in terms of size and mineral content. The limitation with this approach has been the estimation of the model's breakage and liberation parameters.

It was not until a variation on King's (1979) model, which used linear grade measurements, that an accurate prediction of closed circuit behavior was observed. The modification included the addition of a population balance model to create a dynamic simulator which was validated with pilot scale data (Finlayson and Hulbert, 1980).

Recent work at Virginia Tech has lead to the development of a conceptually new modification of the population balance model for grinding. Along with the breakage and distribution relations for all component minerals, a liberation function has been introduced. Image analysis data of areal grade measurements collected on batch mill tests validated the model and the methodology behind the solution of the model parameters (Choi, 1986).

Various methods have been developed for the analysis of mineral liberation. The following section discusses the

evolution in image analysis techniques developed by various researchers.

1.2.3 Quantification of Mineral Liberation

a. Image analysis techniques: Along with the development of models that have liberation terms included, advances in image analysis have given researchers a systematic tool to determine mineral liberation. Data that is acquired for liberation studies is normally taken from polished cross sections of mineral mounts. Prior to image analysis, a variety of different methods existed to quantify mineral liberation these included a linear intercept technique (Rosiwol, 1898), an area tracing technique (Delesse, 1848) and a point counting technique (Thompson, 1930).

An extension of the Rosiwol (1898) method of linear intercepts was used by Barbery (1974) and King (1978) with image analysis to analyze grain sizes. The major limitation of the linear intercept technique is it's inherent assumption that mineral species are isotropic.

Two dimensional area measurements utilize the area of mineral specimens to approximate mineral volumes. The volume percentage of the mineralogical component is taken to be the area of the mineral component divided by the total area of the particle. A method known as "point counting" evaluated the area of mineral components (Thompson 1930).

It utilized a grid of dots which was superimposed over the specimen surface to estimate mineral areas. The area was assumed to be proportional to the number of dots on the mineral surface. A modification of this approach was described by Guadin (1939). Gaudin's technique involved placing a mono-sized mineral specimen in a briquette and treating each particle as having the same size regardless of its appearance. The mineral contents were then estimated as a fraction of the particles total area, thereby eliminating errors associated with the briquette's orientation. Gaudin also included a "locking factor" to make the areal measurement closer to that of actual volumetric values. The "locking factor was used to reduce the overestimation of liberation which arises from observing particles which may only seem liberated. Image analysis equipment allows a more exact estimation of mineral content by actually measuring the relative areas of mineral components. Though image analysis has served to give more exact measurements, it is still limited to either the one or two dimensional approximations.

b. Volumetric Approximation Techniques: In recent years attempts have been made to approximate the volumetric grades from both linear and areal measurements (King, 1982; Bloise et al., 1984). The latest of such attempts has been by the University of Utah. The method developed utilizes a

transformation function to estimate volumetric data from either one or two dimensional measurements (Lin et al. 1986, Miller and Lin, 1988; Lin, Miller and Herbst, 1986). The transformation function is a conditional probability function that is dependent on particle shape and internal grain characteristics such as grade dispersion density and grain size distributions. The matrix has been evaluated using computer simulations of randomly oriented, multiphase, irregularly shaped particles which were generated with a program called PARGEN. This was further followed by comparisons with actual experimental determinations of exact volumetric grades taken from a coarse grained iron ore and a finely dispersed copper ore. The experimental method used to determine the true volumetric distributions involved the sectioning of particles in a systematic way to get several cross sectional views of the same particles. The exact volumetric values compared very favorably to the volumetric transformations of both linear and areal measurements.

The development of models to describe breakage phenomena has allowed researchers to study the effect of breakage parameters in terms of population balance constants. The following section discusses the work that has been done to study the effect of mill operating parameters on size reduction as well as the limited work which has been done on liberation.

1.2.4 Effect of Mill Parameter Changes on Homogeneous Grinding

The major benefits that can be derived from being able to quantify changes in mill parameters and their subsequent effects on the basic grinding model are two fold. Assuming that the population balance constants could be predicted for different mill operating parameters, it would be possible to allow studies on optimization of existing operations. Moreover, the model could be more suited to scale up applications and would replace the "Bond like" approaches that have been used greatly in the past.

As discussed briefly in an earlier section, little work has been done on the effect of mill parameters on liberation and their subsequent role in modeling. In general, the majority of the studies related to mill parameter effects have used homogeneous feeds.

Results from various investigations have concluded that breakage rates in dry batch ball mill experiments are highly dependent on the mill environment and operating conditions. Breakage distribution functions seem to be a material property and are generally considered as being invariant (Herbst and Fuerstenau, 1972). With this in mind, an analysis of breakage rates would yield great insight into mill performance.

The basic grinding equation, though very useful, does not allow for prediction of product size distributions under different mill operating conditions. Experimentally determined model parameters are valid for a constant set of mill conditions.

In an investigation done by Herbst and Fuerstenau (1973), it was concluded that mill speed and mill charge have a great influence on breakage rates; however the resulting changes in breakage rates were energy normalizable. For a variety of different mill speed and mill charge combinations, it was found that plotting the mass fraction of mono-sized feed remaining versus the specific energy input yielded one line, the slope of which was the specific breakage rate s_i^E. A simple modification was then made to the general grinding equation providing the following normalized relation:

$$\frac{dm_i(E)}{dE} = s_i^E m_i(E) + b_{ij}\, s_j^E m_j(E) \qquad [1.7]$$

where the energy specific breakage rates (S_i^E; i=1,n-1) and the set of breakage distribution functions (b_{ij}; j=1,n; i=j+1,n) are approximations of the model parameters which are independent of mill speed, ball load and particle load within normal operating ranges.

The resulting relation was then confirmed by predicting product size distributions for different mill speed, ball load, and particle load combinations. It was also found that the ratio of grinding times needed for the production of the same product size under two different conditions (of mill charge and speed) was equal to the inverse ratio of the specific power inputs.

Other work that has been done in the area of mill filling has determined that increasing the interstitial filling increases the breakage rate up to an optimum, above which a decrease in breakage rates is noted. (Houillier, Neste, and Marchand, 1976) Similar findings have been found with mill speed yielding maximum breakage rates at 70 to 85% critical speed. In order to determine the combined effects of mill operating parameters Forssberg and Zhai (1987) used a factorial design approach to study ball charge, mill speed, feed charge and pulp density on grinding fineness and net energy consumption. Analyzing the derived response surfaces, it was found that charge volume has a significant effect on product fineness and net energy consumption. It was also noted that for a given energy consumption, the importance of operating variables in a decreasing order is as follows: charge volume, feed charge, mill speed and pulp density. Both grinding fineness and energy consumption were found to be very sensitive to charge volume, yet relatively

insensitive to pulp density. Mill speed was found to have a more pronounced effect on fineness than on net energy consumption. Acceptable ranges for ball charge were found to lie from values of 30 to 35% of the mill volume. Mill speed ranges that provided acceptable results ranged from 70 to 85% of critical speed. Volume density ranges varied from 40 to 60%.

Other attempts at studying the effect of mill filling include an investigation conducted by Austin, Smaila, Brame and Luckie (1981). The general objective was to establish a functional form for breakage rates using the fractional filling of balls and the interstitial filling as variables. From batch tests a minimum specific grinding energy was determined by using several combinations of both the parameters studied. Further analysis of the data in terms of specific energy values demonstrated contrary evidence to Herbst and Furstenau (1973). The results indicated that specific energy is not independent of ball load, and that an increase in ball load from 25% to 40% of the mill filling would increase the specific grinding energy 8% while the capacity increased by 16%. The discrepancy was concluded to be possible experimental error on the part of Herbst and Furstenau (1973).

A common finding by various investigators has been that an inverse proportionality exists between a breakage rate

and the corresponding particle loading. This was found to hold true in the case of high mill loads for Gupta and Kapur (1974).

Another operating parameter which has been known to cause significant changes in the breakage rates and overall performance of a ball mill is that of ball size. It is an accepted phenomenon that for every set group of mill conditions there exists an optimum ball size that will yield the greatest breakage rates. In addition, it is also recognized that as particle size increases the optimum ball size increases as does the breakage rate. (Kelsall, Reid, and Restarick, 1968; Kuwahara, 1971) An investigation by Gupta and Kapur (1974) developed a functional relation to predict the effect of ball size on breakage rates. Upon inspection of other work that had been done in the area of ball size effects, the following relation was noted between the selection parameter $S_i(B)$ and the ball size B:

$$\frac{S_i(B)}{S_i^*} = \Phi\left[(B-B^o)/(B_i^*-B^o)\right] \qquad [1.8]$$

where S_i^* is the maximum value of the selection function for the ith size interval corresponding to the optimum ball size B_i^*, and B^o is a constant interpreted as the smallest ball size required to achieve meaningful grinding of the smallest particle size of interest. Φ is a unimodal frequency

function which may be determined by plotting $(B- B^{o})/(B^{*}-B^{o})$ versus S/S^{*}. The resulting curve dictated the choice of a Cauchy distribution and a simple mathematical relation was then developed to predict breakage rates, based on the derived functional relationship. The resulting expression was quite consistent in reproducing breakage rate data that was presented by Kelsall, Reid and Restarick (1968) for quartz in a wet mill.

A similar paper presented by Austin Shoji and Luckie (1976) also provided a functional form to predict the breakage rates attainable under different ball diameters. The technique employed for fitting the data required the introduction of various assumptions so that the estimation method for fitting could be employed. Assuming that the breakage rates attained by a mixture of balls approximates the weighted mean breakage rates of the individual balls, some analysis was done in the predicting of a two compartment cement mill with different ball sizes as compared to a single ball size mill. Using the derived relations, it was predicted that using a larger mix of balls in the first compartment and a smaller mix in the second compartment, would yield a 7% more efficient system than the same amounts of balls in a single mill. It should be noted however, that the original derivations of the relations were

also based on data acquired by Kelsall, Reid and Restarick (1968).

Since both of these papers were based on rather limited experimental data, Gupta, Zouit, and Hodouin (1984) continued the study selecting a variety of different materials including quartz, limestone, soft cement clinker and a hard cement clinker. The first stage of the project was to determine the error associated in mill scale up by manipulating the mill diameter and the corresponding ball size. Extensive errors were incurred when scaling up to a 3 meter mill from 10 and 15 inch mills. Error factors of as large as 1.75 were obtained in the approximation of breakage rates. This yielded ranges from 43% lower to 75% higher values than the correct values. The large fluctuations were due to the accuracy of the original breakage rate estimates encompassing anywhere from 5 to 10% error. In order to minimize the errors the mineral was preground and more care was taken to ensure a closer size range in the batch mill feed. The functional forms developed included constants that were material independent and predicted breakage rates in 90% of the cases that were within 1% error of actual experimental values. In all the cases studied, different materials yielded radically different values for the material constants. Therefore, it was concluded that a general equation proposed by other researchers is not

possible since different materials react differently to ball size and mill size changes.

It should be noted that even though the majority of the ball size experiments have been conducted on single ball size loads, industrial operations involve a distribution of ball sizes. This could be responsible for some of the significant errors associated with population balance scale up values. With this in mind a recent study by Lo and Herbst (1986) utilized a distribution of ball sizes in hopes that it would improve the accuracy of scale up predictions. Their experiments were conducted using choices of mill speed, ball load, particle load, solid percentage, and ball size distributions that are typically used in industry. A procedure was developed that allowed laboratory experiments to be performed with the same ball size distribution as that of a plant. The procedure involved plotting the energy specific breakage rate versus the particles size for each ball size distribution. The resulting curves intersected at one pivot point with each type of material. These values were then utilized to develop functional relationships which predict the energy specific breakage rates at various ball sizes. Breakage distribution functions were observed to change only slightly with ball size. This allowed initial estimates of distribution functions to be used regardless of

a change in ball size. The resulting predictions for the variety of minerals tested provided excellent results.

Most of the grinding experiments that have been conducted have been dry batch tests. In the case of wet grinding, it has been noted by several researchers that breakage rates significantly increase for the larger size classes. This general trend is not as prominent for smaller size classes (Fuerstenau and Sullivan, 1962; Berube, Berube, and Houillier, 1979). Another well know phenomenon is the inherent increase in the breakage rates with time for wet grinding. Though these breakage rates could be fitted with empirical relationships, the resulting values would have no true physical significance in as far as the classic grinding model is concerned. In order to analyze breakage rates the initial slopes of the disappearance plots have been taken to be the representative values. (Tangsathitkulchai and Austin, 1984)

1.3 RESEARCH OBJECTIVES

The objective of the present investigation is to develop a general understanding of how changes in ball mill parameters affect breakage rates of liberated and composite particles. The eventual goal of this study is to see if liberation can be affected independently of size reduction. If this were in fact the case, then mill design could be improved on the basis of liberation. Though this study is fundamental, it is hoped that it will yield a valuable insight into the breakage characteristics of composite minerals and a conceptual grasp of how mill parameters may affect liberation.

All breakage rates are analyzed in terms of energy normalized values (Ton/kw hr). The normalization or non-normalization of breakage rates will yield clues as to which breakage rates will require functional forms in terms of a liberation model. As noted in the literature review, previous work has been limited to studies on homogeneous material. Though the past information gathered is helpful, it does not address the key role of grinding which is liberation. It is for this reason that this project has been designed to study the effect of mill speed, ball size, mill charge and wet vs dry grinding with particular emphasis on the breakage of composite particles. It is hoped that the information gathered can act as a precursor in the

development of a liberation model that predicts both mineral product size and the degree of liberation attainable under varying mill operating conditions.

CHAPTER II.

EXPERIMENTAL PROCEDURES

2.1 **Ore Sample**

The ore sample used for this investigation was basically a binary ore composed of coarse grained sphalerite and dolomite. Its coarse liberation size simplified the analysis of the mineral system by image analysis. Furthermore, the relatively large contact zone between both mineral species, was desirable in studying liberation. It was acquired from ASARCO's Young Mine which is located in Jefferson City Tennessee. The processing plant treats approximately 7,700 tons/day of ore. The ore itself has a grade of approximately 3% zinc. The preparation stages involved at the sight include two stage crushing, heavy media separation, followed by ball milling and finally a flotation circuit.

The heavy media separation device, which uses ferrosilicon, processes 250 tons/hr of ore. The basis for this technique utilizes differences in the specific gravities of sphalerite (4.0 SG) and dolomite (2.8 SG). The heavier ore particles containing sphalerite sink while the lighter particles float yielding nearly 77% of the dolomite dominant particles as tailings.

The total sample weight which was acquired was 1500 lbs of concentrated ore from the heavy media circuit containing nearly 14% zinc. The sample consisted of particles that were 2 to 3 inches in size.

2.2 **Grinding Equipment and Torque Measurement**

The batch grinding experiments were conducted in a stainless steel mill measuring 25.4 cm in diameter and 29.2 cm in length, with lifters spanning its length. The mill rested on roller bearings and was connected to a .5 horse power electric motor. The shaft which linked the two had a Brewer Engineering Laboratories model A-055 torque transducer. The output from the torque transducer was displayed on a Brewer Engineering Laboratories model DJ-335A/2 digital readout sensor.

The mill's operating characteristics are described by Yang et al. (1968). The balls used in the mill varied from 3/4-inch, 1-inch and 1- 1/4-inch balls, the weight of which in all cases was approximately 30 Kg. The volume filling of the balls occupied approximately 50% of the mill.

2.3 **Sizing Equipment**

Standard eight inch diameter Tyler series sieves ranging from 10 to 400 mesh were used in combination with a model B Ro-Tap machine. A Mettler AC 100 balance was

employed to measure weights providing an accuracy of $\pm$ .01 grams. It should also be noted that a standard wet screen shaker was used to perform a more efficient wet screening.

2.4 **SEM-IPS Image Analyzer**

A Kontron Scanning Electron Microscope-Image Processing System (SEM-IPS) was used to collect image analysis data (see Fig. 2.1). This system was designed to either acquire images from an energy dispersive SEM or from a video input which monitors a mineralogical microscope.

The following is a list of the actual hardware which made up the system: Zilog Z80A (4MHz) processor with 64 KByte dynamic system RAM, 8 Bit data bus, 16 Bit address bus, 20 MByte Winchester hard disk, 600 KByte Floppy disk, CRT controller for alpha and graphic monitors, 2 serial ports RS-232-C, slow scan interface, scanning stage interface and an autofocus interface.

The actual image processor unit had the following specifications: array processor with pipeline structure, hardware multiplier, 16 Bit ALU and 6 KByte microprogram memory, 8x256 KByte image memory, additional 2 MBit for overly or parity, variable format image storage, standard 512*512 pixels at 256 grey level values plus 1 bit parity, and a A/D converter for the TV-signals. The high resolution

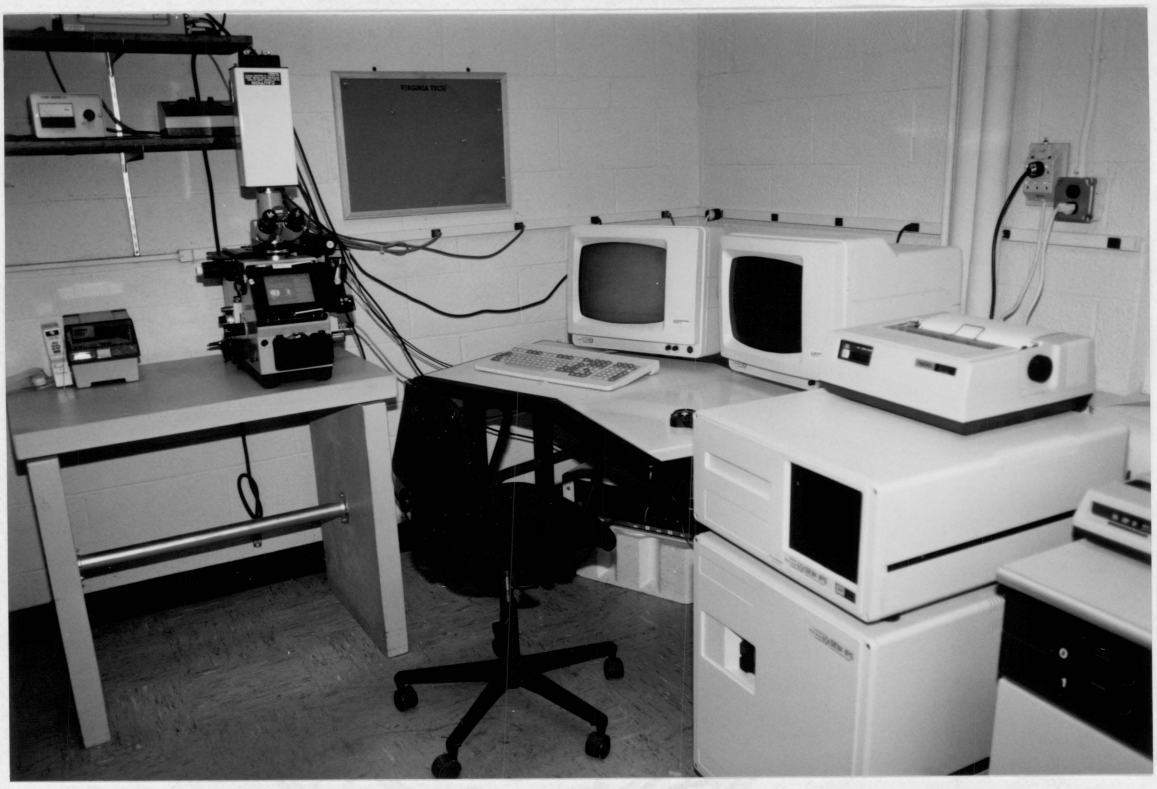

Figure 2.1 SEM-IPS image analyzer.

color monitor had a band width of 20 MHz (+/-3db), 800 lines / 50Hz or 640 lines / 60Hz.

Commands, program listings, and graphics were displayed on a black and white monitor. Access to program commands was achieved by an ASCII keyboard and a digitizer tablet with a crosshair cursor. Hard copies of data, graphics or program listings could be made with a OKIDATA, Microline 82A printer.

The actual image source for the experiments conducted came from a Zeiss Inverted Camera Microscope, type 405. The link between the microscope and the SEM-IPS system was a Dage MTI 86 Series mounted television camera.

The IPS software available for this system allowed enhancement of images and processing of data. It also allowed the distinction of objects on the basis of grey levels as well as geometrical shapes. Whichever the method of distinction used, the final objective of the system was to separate the objects to be studied from the background. This process, which is termed discrimination or segmentation, is normally done by grey level threshold values which the operator has designated. Pixels that fell into the selected grey level ranges were converted to a binary 1. All other pixels, which were not in the specified range, were converted to binary 0. This binary image assumed a black and white color with the objects of

interest. This image was then used to provide either field or object-specific measurements.

Discrimination was facilitated by a variety of image processing procedures such as spatial filtering, contour enhancement, shading corrections, etc.. After the image had been discriminated, further processing of the image eliminated errors due to noise. A criteria was then used to selectively choose particles on the basis of size or shape. It was also possible to interactively edit grey levels on the created binary images.

All changes that were affected by the processing commands were evident on the high resolution screen. The actual commands were depicted on the host processor monitor which had a menu that allowed access to all the processing routines. To select an image processing routine a mouse was utilized which moved a cursor throughout the screen. Input variable numbers were entered with the keyboard.

The variety of functions chosen were all storable as a program. Once established, a program was executable with a single command.

2.5 **Experimental Procedure**

2.5.1 Sample Preparation

The ore which was acquired from the mine measuring approximately one to three inches in size was passed through

a 5x6 inch laboratory jaw crusher. This material was then passed through a 8x6.5 inch hammer mill so that the final product size was -10 mesh. Narrow size fractions were then prepared by sizing the hammer mill product.

2.5.2 Grinding Experiments

The ball mill used to do all the batch grinding experiments for this study is described in section (2.2). In order to study the effect of mill speed, tests were conducted at 40 and 85% of critical speed. In each of these cases, a 1 inch ball size diameter and a feed of 3000 grams was used. The closely sized feeds were ground dry for 1, 2 and 4 minute intervals. In studying ball size, a 75% critical speed was used for all the tests with a charge of 3000 grams per test. Ball size tests of 1, 2, and 4 minutes were conducted for each of the ball sizes of 3/4, 1, and 1-1/4-inch diameter. Mill charge tests were conducted at 75% critical speed with a 1-inch ball size for each of the charges of 3000, 4500, and 7100 grams. With the exception of the 3000 gram charge which was conducted for 1, 2, and 4 minute intervals, the remainder of the experiments were conducted only at 4 minutes to conserve material.

At the end of each grinding time, the mill was kept stationary to avoid the loss of fines when opened. The mill was then emptied and special care was taken to collect all fines adhering to the mill. All samples weighing 4500 grams

or less were then split into eight portions. The 7100 gram run was split into sixteenths due to the large amounts of material present in each size class. These splits were then weighed and later dry screened on a Ro-Tap sifter for a duration of 15 minutes, to produce size fractions ranging from the top size class down to -400 mesh material. Dry screening was then followed by wet-screening to remove fines from each of the classes. The material which passed during the wet screening was then added to the next size class down to avoid loss of material. The loss of material never amounted to more than .1% of the total charge. The samples were then dried, weighed and bagged for later use in the preparation of briquettes.

2.5.3 Briquetting and Polishing

Material from each size fraction of interest was representatively split into approximately 10 gram samples and added to 1 inch diameter molds. Cold setting EPOFIX Epoxy was then added to the mold and the briquette was placed under a vacuum in order to remove excess air bubbles. The mold was then allowed to sit overnight. Once the epoxy had hardened, the briquettes were then cut into 5 vertical cross sections using a Buehler Isomet Low Speed Saw. These slices were then remounted in epoxy resin and allowed to harden. This procedure was implemented to avoid orientation

effects which have been found to cause error in previous studies.(Choi, 1986).

The particle mounts were then polished by using a 600-grit metal- bonded diamond lap followed by polishing on a canvas using 600-mesh silicon carbide as an abrasive. The final stages of polishing included the use of 6-micron diamond paste on a TEXMET pad, followed by the use of a Syntron Auto Polishing machine with .05 micron alumina powder for a period of 10 hours.

2.5.4 Liberation Analysis

In general the image processing procedure can be illustrated by Figure 2.2. An analog image from the microscope was digitized on the high resolution monitor. The image was then enhanced and processed in order to facilitate the accurate extraction of the objects of interest. Once extracted the defined objects were then converted to binary images of white on a black background. At this stage the area measurements could be made on the selected objects in either an object or field-specific manner.

In order to obtain liberation data, the polished briquettes were analyzed using the SEM-IPS image analysis system. The system was used to provide areal grades of each particle. Areal assay data from each particle was printed out and stored on a floppy disk.

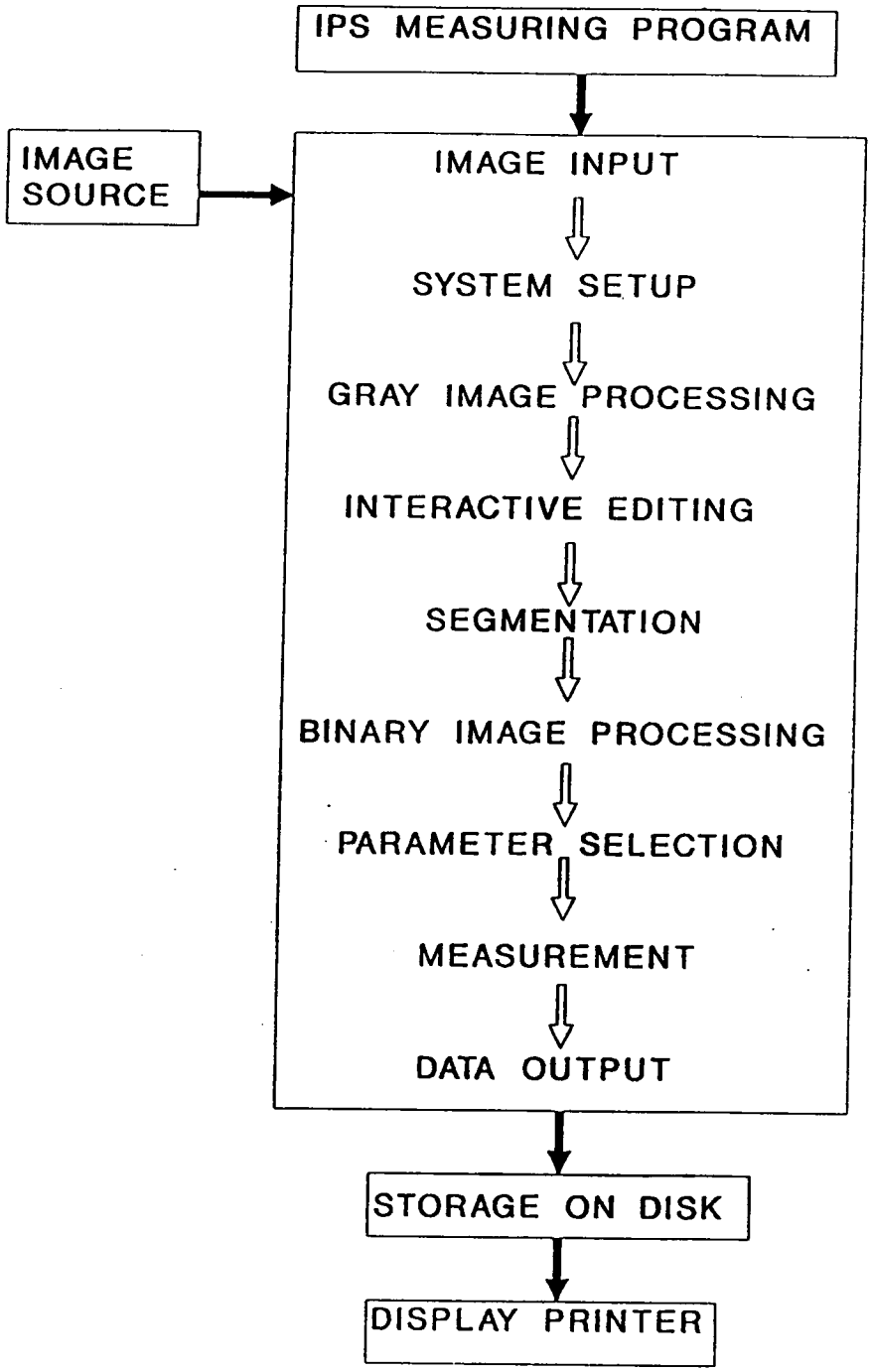

Figure 2.2 Image Processing Procedure

An attempt was made to implement the transformation program developed by Lin (1985) to convert the areal data to volumetric approximations. The output from the program provided results that were not credible or physically possible. In addition to providing negative values for masses in certain grade classes, some grade classes were reported to have more mass after a 2 minute grind than a 4 minute grind. These discrepancies could be attributed to the small amount of material that was associated with the problematic grade classes. In general, the program seems to be limited to mineral systems that have an even distribution of grade classes.

With the absence of an adequate volumetric approximation technique, the areal values were taken to be equivalent to volume. All the particles were presumed to be the same size in the measurement of areal percents regardless of the apparent size under the microscope. This assumption was taken since each briquette was composed of closely sized material. The free particles observed were taken to be liberated material and were not corrected by the use of locking factors. The weight fractions of each particle class were then obtained by multiplying by the specific gravity of each component. The mass ratios of each class could then be obtained by using a simple program to selectively keep track of masses in terms of predesignated

grade classes. In order to have a larger number of observations per class, the ranges of 0-5%, 5-50%, 50-95%, 95-100% sphalerite were used to quantify the distribution. The two extreme cases of 0-5% sphalerite and 95-100% sphalerite, were assumed to act as liberated material for the purpose of data analysis.

2.5.5 Statistical Analysis

The two types of error associated with image analysis measurements are that of operator error and statistical error incurred if too few particles are counted. The error which is due to the operator is significantly reduced with experience. Statistical error can be evaluated with a statistical analysis described by Jones (1982) and Lin et al. (1985). This same method may be employed to determine the amount of particles required to acquire an unbiased representative sample of a real or linear grade distribution.

Since particles are randomly distributed in the epoxy matrix, the best estimate of the density in the i-th grade interval (f_i), and the relative error (S_i) may be described by the following relation:

$$f_i = \frac{\sum_{j=1}^{n_i} W_j}{\sum_{j=1}^{n} W_j} \times 100 \qquad [2.1]$$

and

$$S_{fi} = \frac{f_i}{\sqrt{n}} \qquad [2.2]$$

where

n = total number of observations

n_i = number of observations in the i-th grade interval

W_j = weighting factor for a given observation: $W_j = 1$ for the measurement based on number, $W_j = l_j$ for the measurement based on length where l_j is the intercepted length of particle j.

f_i = percentage in the i-th grade interval

S_{fi}= standard deviation which is the expected accuracy of the analysis of the percentage in the i-th grade interval

Equation [2.2] may be used to establish the smallest number of observations required to produce accurate estimates of volume fractions of the components. If the number of composite particles amount to 10% of the total volume and are randomly distributed within four grade intervals, then $f_i = 2.50$. For an expected accuracy of 5% (S_{fi}=.05), the minimum number of observed particles would be:

$$n = \left(\frac{f_i}{S_{fi}}\right)^2 = 2500$$

With this calculation in mind, particle counts were maintained at 2500 and above to ensure precise measurements for all the experiments conducted.

CHAPTER III.

EXPERIMENTAL RESULTS

In order to establish breakage rates a sequence of batch grinding experiments were conducted on a coarse grained sphalerite ore. The breakage rates for particles with different sphalerite content were evaluated with an SEM-IPS image analyzer.

3.1 **Comparison of Image Analysis Results Against Chemical Assays**

Table 3.1 illustrates the assay results from image analysis and chemical assays and the relative error between both for two sample specimens. The procedure used for chemical analysis is located in Appendix V. It should be noted that quite accurate results can be obtained with image analysis techniques.

TABLE 3.1 Comparison of the zinc content determined with image analysis and chemical assays.

Size (mesh)	Image Analysis (X1)	Chemical Assay (X2)	Error*
10x14	8.85	8.54	3.63
14x20	14.43	13.44	7.37

$$*\text{Error} = \frac{X1-X2}{X2} \times 100$$

The slight overestimations of grades with image analysis can be attributed to the lack of locking factors. Some of the particles observed may have seemed liberated due to their orientation, when in actuality they were locked. Nevertheless, the close approximations of areal grades to chemical grades verifies the accuracy of the sample preparation and the experimental procedure involved in this study.

3.2 **Feed Characterization**

An example of a feed characterization for one of the narrowly-sized feeds used is illustrated graphically in Figure 3.1. The characterization data for all the feed samples are located in Appendix I under Tables I-1 through I-10. For the purpose of analysis, material that contained less than 5% or greater than 95% sphalerite was assumed to act as free material. It should be noted that the majority of the feed material was already free leaving only approximately 10% of the material as composite particles. This liberation phenomenon can be explained by the large grain size which is inherent in this mineral system.

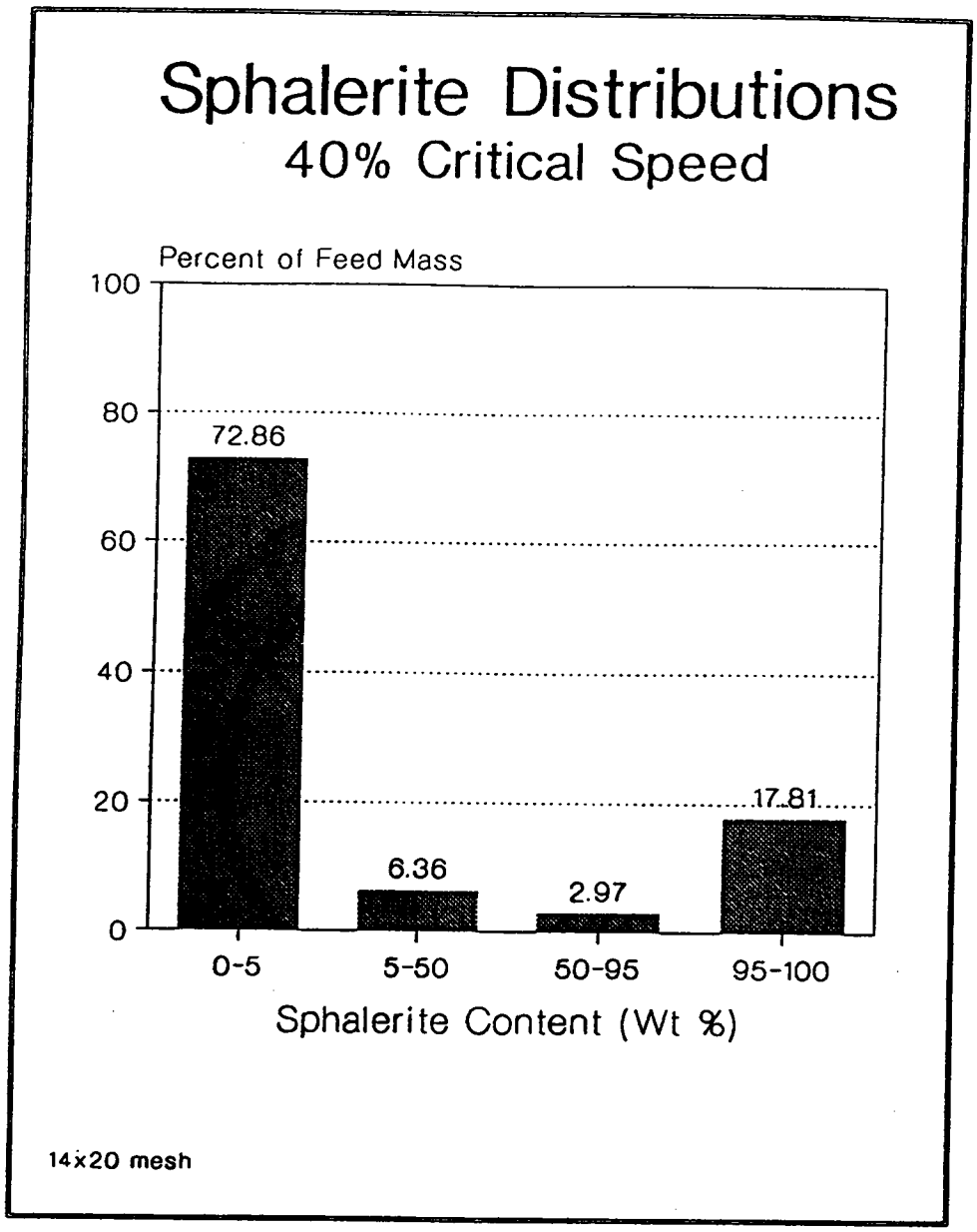

Figure 3.1 Example of a 14x20 mesh feed distribution for a 40% critical speed test.

3.3 Determination of Breakage Rates

The top feed size breakage rates (selection functions) for liberated and composite classes may be determined by the disappearance of this material from the original narrowly-sized feed. Since material can only break into smaller sizes, it is possible to plot the fraction remaining verses time for a given feed composition. Since the amount of material which is liberated and composite can be quantified by image analysis, a single series of grinding tests can provide breakage rates for all classes of particles.

The determination of the top size breakage rate for a particle class of composition x is carried out by grinding the total ore in a batch mill. In this example, $m^x_1(0)=1$ and $m^x_i = 0$ for i=2,....N. Equation 1.2 then becomes:

$$\frac{dm_1^x}{dt} = S^x_1 \cdot m^x_1(t) \qquad [3.1]$$

where m^x_1 is the mass of material that is of size class 1 and a composition of x.

Solving for the breakage rate of size 1 and composition x:

$$-S^x_1(t) = \ln \frac{m^x_1(t)}{m^x_1(o)} \qquad [3.2]$$

Thus the slope of a plot of $\ln[m^{x}_{1}(t)]/m^{x}_{1}(o)$ versus time which by convention is know as a disappearance plot, is equal to $-S^{x}_{1}$.

Figure 3.2 is an example of a typical disappearance plot. The disappearance plots for the various experiments conducted under different operating conditions are located in Appendix III. Included in these illustrations are plots for material that ranges from 0-5%, 5-50%, 50-95%, and 95-100% sphalerite. In general, the disappearance plots were either first order with some data scatter, or concave (indicating a decreasing breakage rate with time). Therefore, initial breakage rates were used whenever possible to compare the various conditions studied. The distributions acquired for all the experiments are located in Appendix I under tables I-1 through I-10. The actual calculated percent remaining values that were plotted are located in Appendix II under tables II-1 through II-10.

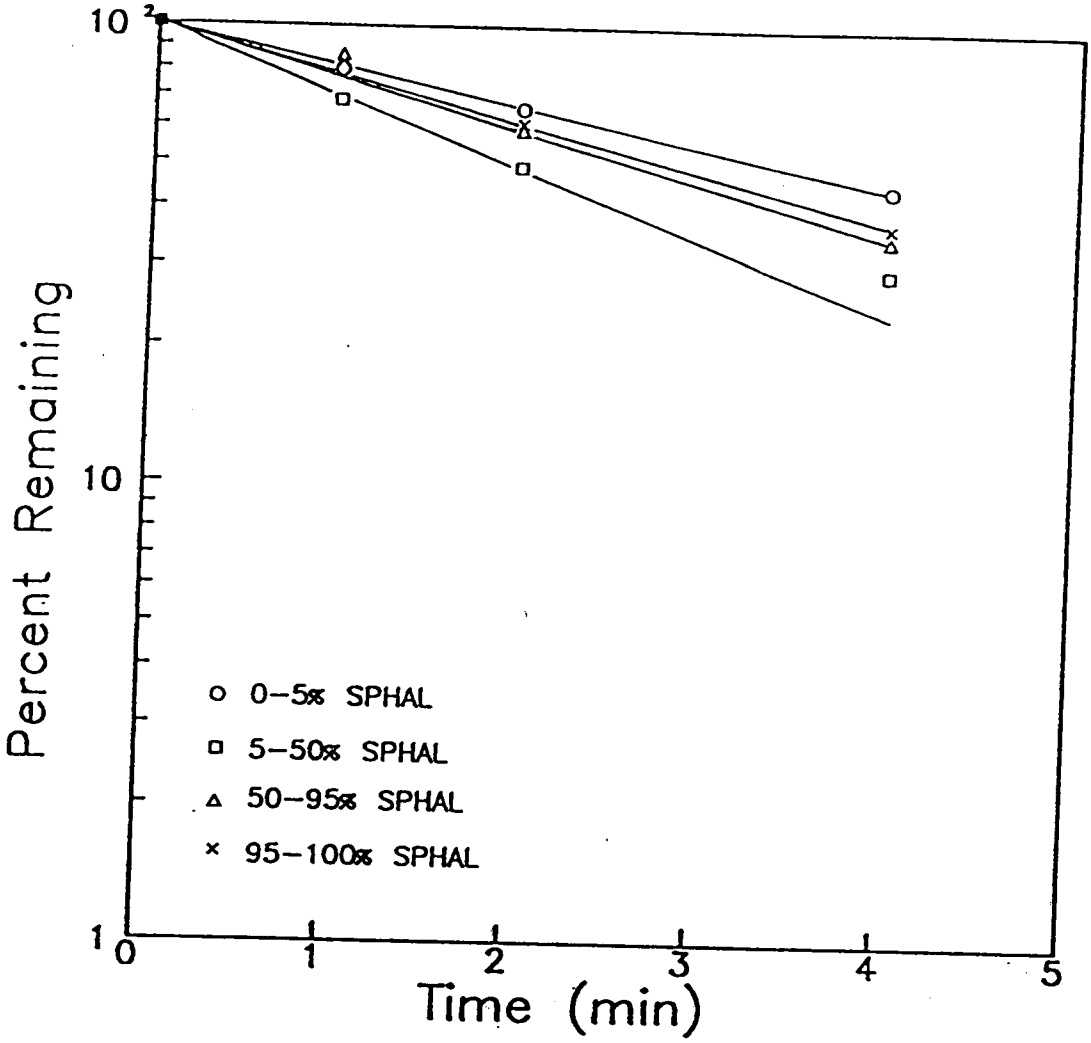

Figure 3.2 Example of a disappearance plot for 14x20 mesh feed at 40% critical speed.

3.4 Determination of Energy Specific Breakage Rates

In order to determine Energy Specific Breakage Rate values, the following relationship was employed:

$$SE = S\ H/P\ (60min/1hr)$$

where

SE = Energy Specific Breakage Rate (Tons/kWhr)
S = Breakage Rate (1/min)
H = Hold Up in Mill (Tons)
P = Power (kW)

The displayed torque values in inch-pounds and the corresponding revolutions per minute were used to calculate the power applied to the shaft via the following relationship:

$$P = (2\pi n)\ T$$

where
P = Shaft Power Input (in-lb/min)
T = Torque (in-lb)
n = Revolutions Per Minute

Converting to Kilowatts, the equation becomes

$$P = 1.182 \times 10^{-5} Tn$$

where

P = Shaft Power Input (kW)

The conversion of the mill hold up from grams to tons is as follows:

$$H = (\text{feed in grams}) \times 1.10229 \times 10^{-6}\ \text{Tons/gram}$$

The values obtained for the calculated breakage and energy specific breakage rates are located in tables IV-1 through IV-4 in Appendix IV. The following section attempts

to quantify the effect of experimental error on these calculated values.

3.5 **Effect of Image Analysis Error on Breakage Rate Calculations**

In order to quantify the effect of image analysis error on Breakage rate calculations, particle counts for a 10x14 mesh sample were varied in increasing order of abundance up to 3000 particles. The resulting weight percent fractions for each class were compared for 2000 and 3000 counts. Table 3.2 illustrates the results obtained and the relative error between both initial breakage rate estimations.

TABLE 3.2 Effect of Image Analysis Error on Areal Grades.

Particle Class	%BY WEIGHT OF TOTAL MASS 2000 Particle Counts (X1)	3000 Particle Counts (X2)	Deviation From Mean	Relative* Error
0-5%	81.34	81.11	.115	.14%
5-50%	6.97	7.68	.355	4.85%
50-95%	3.09	2.60	.245	8.61%
95-100%	8.59	8.60	.005	.06%

*Deviation From Mean = ABS(X1-X2)/2

$$*\text{Relative Error} = \frac{\text{ABS}(X1-X2)/2}{(X1+X2)/2} \times 100$$

The 3000 particle count sample was taken to be the most accurate approximation, thereby allowing an evaluation of

the error taking a conservatively lower number of particle counts (ie. 2000). It should be noted that the liberated mineral components have negligible error and therefore require much fewer particle counts to get accurate weight percent approximations. Table 3.3 illustrates the error associated with calculating breakage rates for an experiment conducted at one, two and four minutes at 40% critical speed with a 1" ball size and 65% interstitial filling. The values of "deviation from mean" in table 3.2 are either added to, or subtracted from, the weight percent values to give positive or negative error values, respectively.

TABLE 3.3 Analysis of Error Associated With Image Analysis in the Calculation of Breakage Rates.

Particle Class	Calculated Breakage Rate With Negative Error	No Error	Positive Error
0-5%	.2022	.2016	.2010
5-50%	.3583	.3546	.3510
50-95%	.2670	.2652	.2634
95-100%	.2495	.2595	.2494

Even though image analysis was expected to be the primary source of error, it can be seen by table 3.3, that very little error was introduced even if a conservatively small number of observations are taken. It should be noted that the rest of the experiments conducted in this investigation were also expected to behave in a similar manner.

The calculation of energy normalized breakage rates involves the measurement of both the revolutions per minute as well as the torque. From the standard deviations that were incurred, it is estimated that the error associated with these measurements did not exceed 1.3%. This small amount of error would have very little effect on the calculated energy specific breakage rates.

CHAPTER IV.

DISCUSSION OF RESULTS

4.1 **Analysis of Breakage Rates**

To simplify the analysis of the breakage rates in terms of composition and operating parameters, plots have been generated in which the breakage rates have been plotted versus the percent sphalerite class for each parameter. The mill speed parameter for 40 and 85% critical speed is illustrated in Figure 4.1. These values were chosen since 75% critical speed represents a normal operating condition of a ball mill and the other two values would be considered extreme operating conditions of cascading and cataracting environments. From this plot it can be noted that the 85% critical speed provides the greatest breakage rate for all the particle classes. In going from 40 to 85% critical speed there is a shift in the optimum breakage rate for composite classes from 5-50% sphalerite to 50-95% sphalerite. This shift could be attributed to the actual kinetics within the mill changing from a predominantly cascading environment to one which has a cataracting zone. This would tend to indicate that the material which consists of 5-50% sphalerite is more apt to break preferentially faster under attrition conditions than the 50-95% sphalerite material which is more apt to break faster under impact

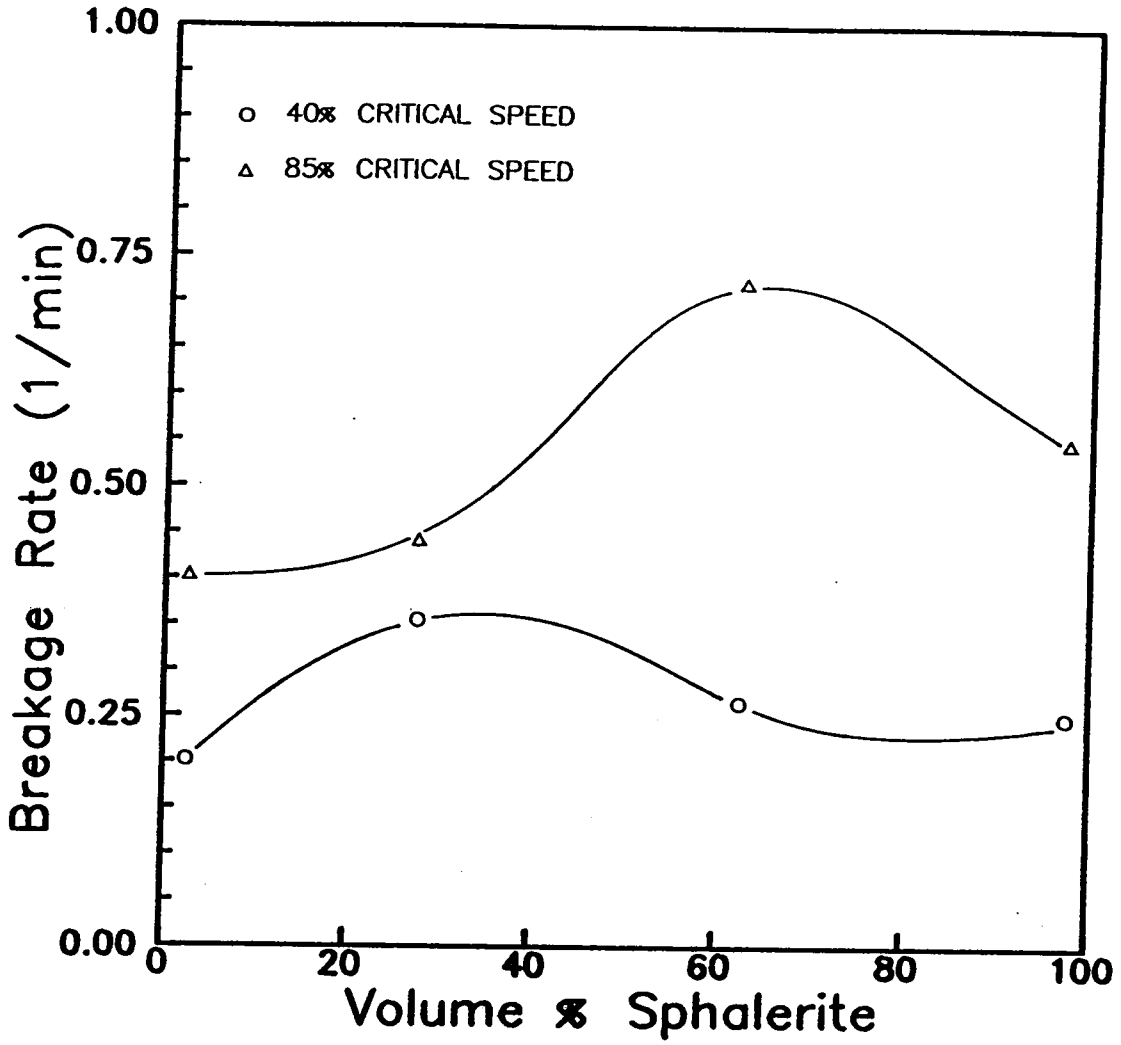

Figure 4.1 Breakage rate versus percent sphalerite plots for different mill rotational speeds with 14x20 mesh feed.

conditions. This phenomenon could be explained by the fact that sphalerite is more brittle and therefore is more apt to break under cataracting conditions. It follows that particles which have a higher sphalerite content would tend to break preferentially in a cataracting environment. This is also supported by the fact that the increase in breakage rates, associated with an increase in mill speed from 40 to 85% critical speed, is more prominent for sphalerite rich material.

In analyzing the effect of ball size, Figure 4.2 shows that a 1- inch ball size is the most effective in reducing 10x14 mesh feed for all composition classes. It is also apparent that the breakage of classes consisting of greater than 50% sphalerite are significantly enhanced with the usage of the 1 or 1 1/4 inch ball sizes. This increase in breakage rates is much less apparent for material consisting of less than 50% sphalerite, indicating that the degradation of dolomite is less susceptible to a change in ball size. A possible reason for this phenomenon is that the ball-ball interaction or energy input due to friction remains relatively similar, while the impact energy of cataracting balls changes greatly with different ball masses. This once again supports the contention that sphalerite rich material seems to exhibit improved breakage under impact conditions.

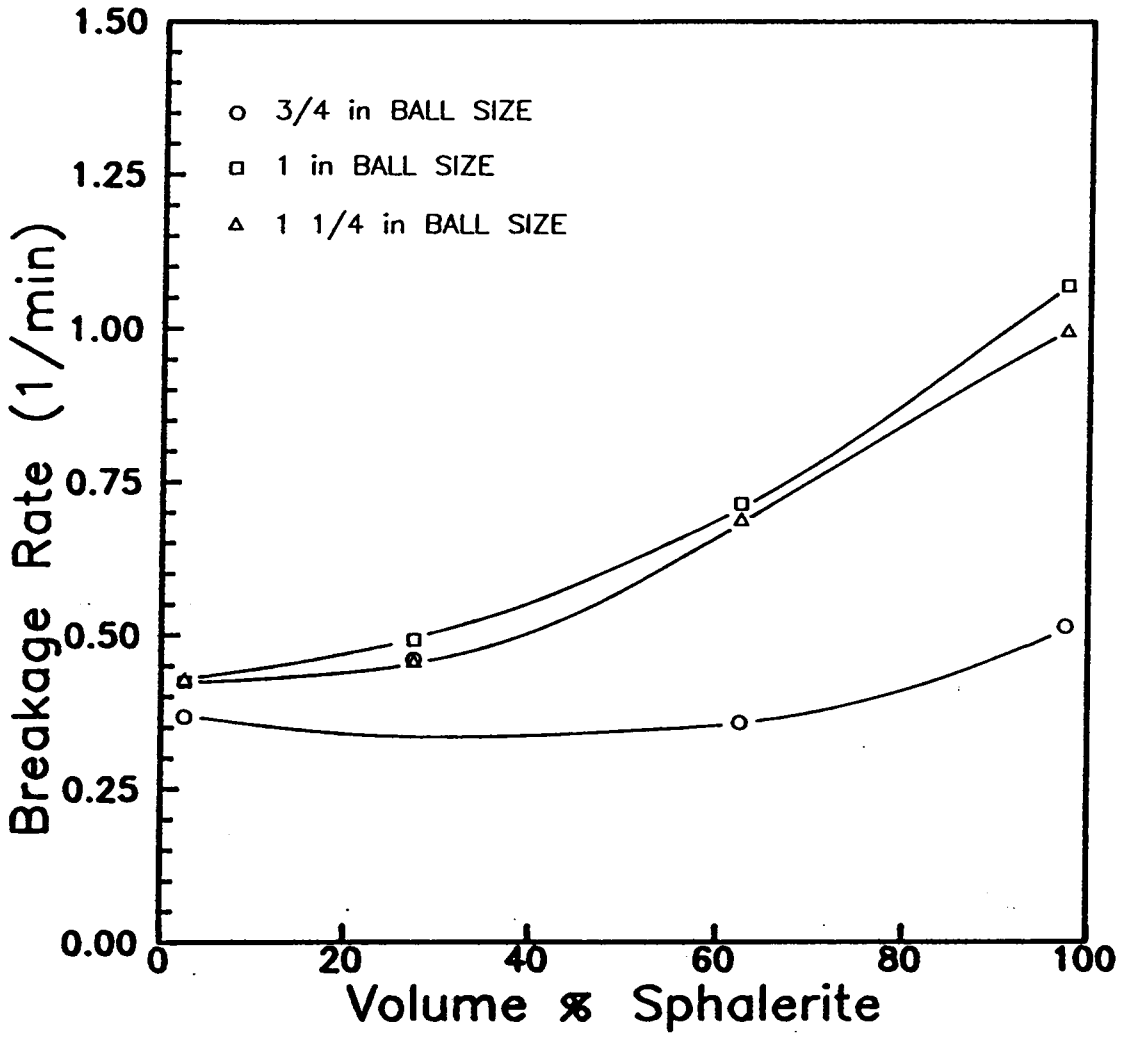

Figure 4.2 Breakage rate versus percent sphalerite for various ball size diameters with 10x14 mesh feed.

It is also interesting to note that an increase of ball size to 1 1/4" provides similar values of breakage rates as the 1" ball size. This would tend to indicate that the true optimum ball size could be between 1" and 1 1/4" diameter. Impact energy seems to be a function of both momentum and contact area. Increasing or decreasing the ball size from the optimum value, has a detrimental effect on impact energy by influencing momentum and contact area accordingly.

The effect of mill charge yielded similar results to the other parameters in that an optimum value of interstitial filling was found that resulted in enhanced breakage rates for all compositions of particles (see Figure 4.3). An interstitial filling of 65% was found to be the most efficient in breaking 10x14 mesh material with a 1" ball size. Increasing the amount of charge to 150% interstitial filling decreased all the breakage rates and had an even more significant effect on the composite classes. At 150% interstitial filling the composite classes had lower values of breakage rates than either the dolomite or sphalerite. This would tend to imply that an overcharging of the mill impedes the breakage of composite materials as well as sphalerite. The possible cause for the lessening of the breakage rates is the cushioning effect of the excess mineral and its associated reduction of impact energy to particles. It is of great interest that this

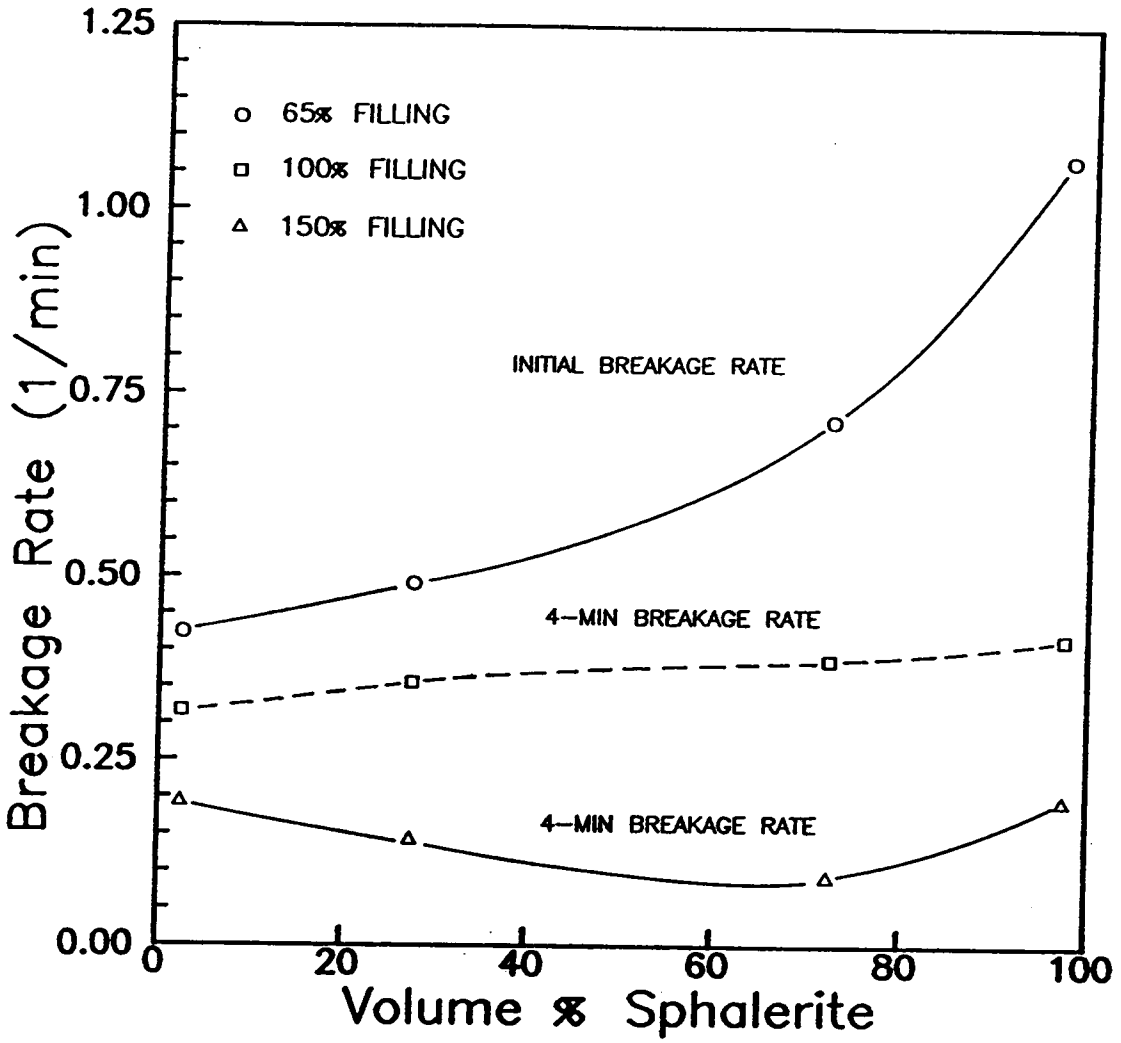

Figure 4.3 Breakage rate versus percent sphalerite for various interstitial filling with 10x14 mesh feed.

cushioning effect seems to be more effective with particles containing sphalerite since this would indicate that these materials are more susceptible to impact than liberated dolomite.

Comparing 4 minute grind data, wet grinding provided enhanced breakage of the 14x20 mesh feed in all the composition classes, as can be seen in Figure 4.4. A possible reason for the enhancement of breakage rates is the inherent suspension of fines within the wet environment at 70% solids. It should be noted that the general increase in breakage rates was more prominent for the classes containing sphalerite, once again indicating that this material may be more susceptible to impact conditions.

The lack of curvature on the dry grind can be attributed to the fact that only 4 minute grind data was available due to a shortage of 14 x 20 mesh material. With this in mind, only the 4 minute grind data was used for the 70 percent solids plot.

4.2 **Analysis of Energy Specific Breakage Rates:**

Since all of the parameter changes involved a change in the energy draw from the mill, the breakage rate values were normalized with respect to energy to see if the actual breakage kinetics were changed as opposed to the changes being simply a function of energy input. Plotting the

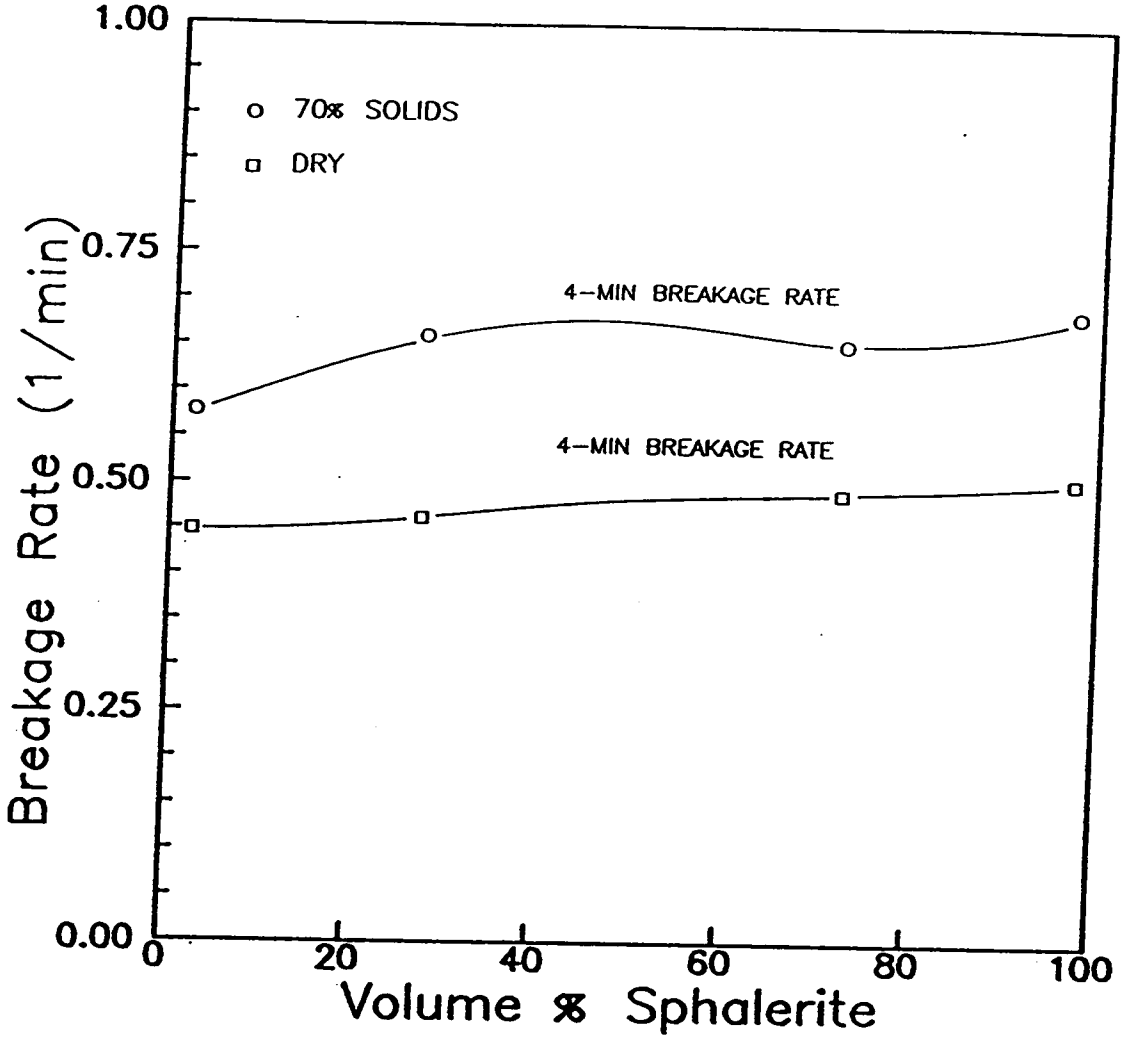

Figure 4.4 Breakage rate versus percent sphalerite for dry and 70 percent solids grinding environments with 14x20 mesh feed.

specific breakage rate versus the percent sphalerite, allows the analysis of parameter changes in terms of energy normalized breakage rates for each composition class.

Figure 4.5 illustrates the effect of a change in mill speed on the energy specific breakage rates of 14 x 20 mesh material. Once normalized with respect to energy, the free sphalerite and dolomite components move much closer together, however the composite classes still exhibit their differing peaks. This indicates that changes in the mill rotational speed could be considered energy normalizable for the free components. If this were in fact the case, a general liberation model could use a simple energy relation to describe free particle breakage and a functional relation to describe composite particle breakage.

A change in ball size yields values for specific breakage rates that vary greatly when an optimum ball size is used. The effect of ball size on energy specific breakage rates can be seen on Figure 4.6. The 1" and 1 1/4" ball sizes seem to normalize with respect to energy, while the 1/4" ball size diverges from the larger ball sizes. A possible reason for the apparent normalization of the two larger ball sizes could be that the optimum ball size range is sufficiently large to provide similar breakage rates for both sizes. Since the power draw for both of the larger ball sizes were similar, it follows that the energy specific

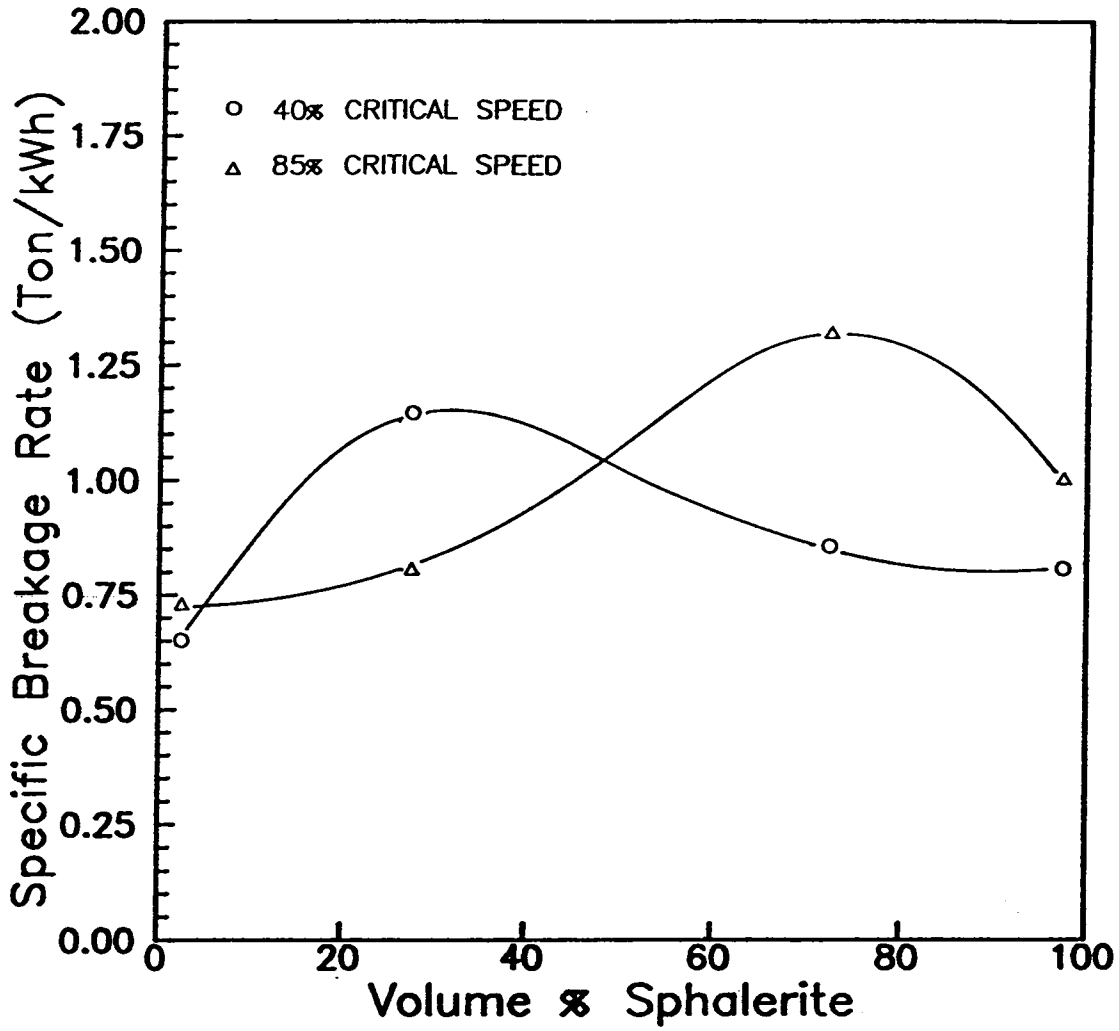

Figure 4.5 Energy normalized breakage rates versus percent sphalerite for different mill rotational speeds with 14x20 mesh feed.

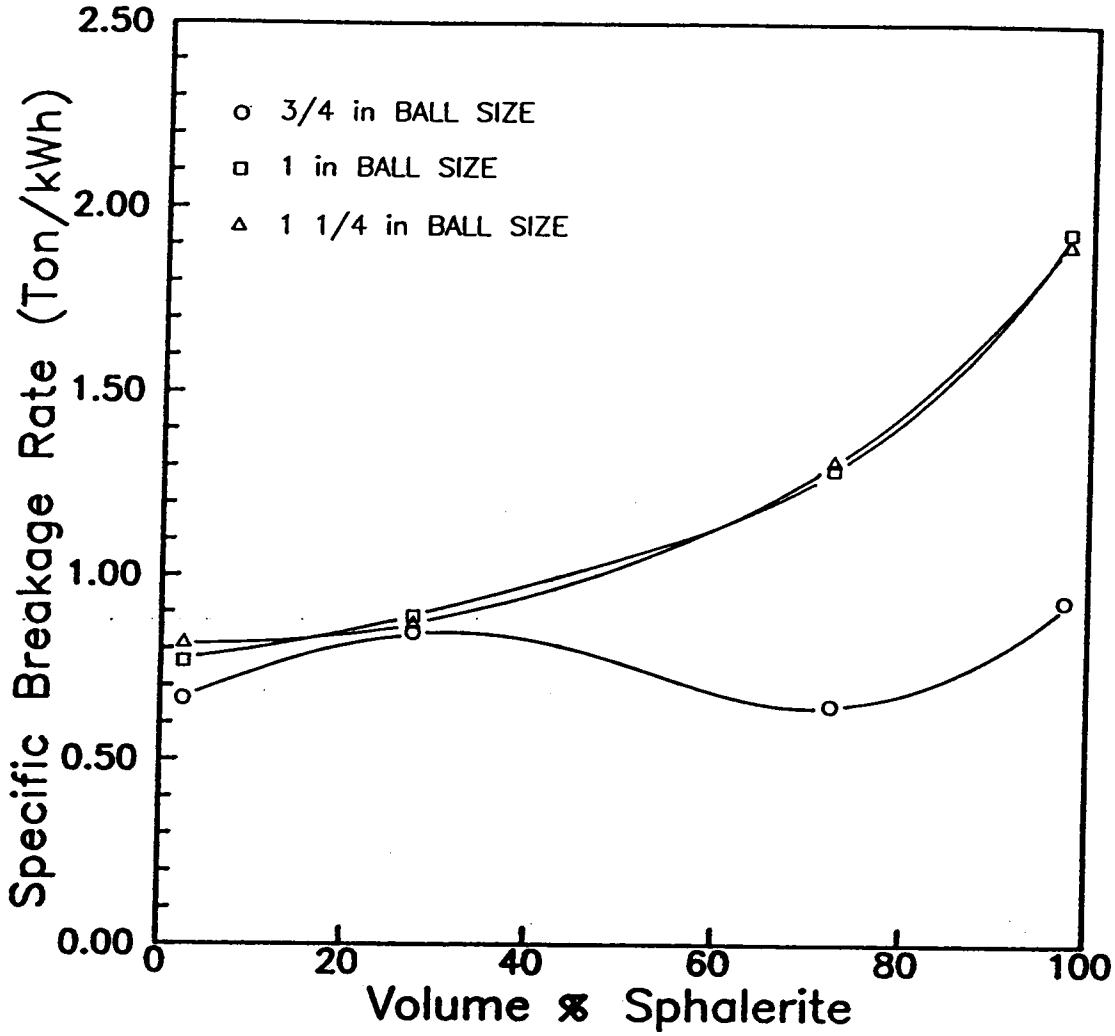

Figure 4.6 Energy normalized breakage rates versus percent sphalerite for different ball sizes with 10x14 mesh feed.

breakage rates would be comparable in magnitude. Nevertheless, the divergence of the 1/4" ball size indicates that ball size is not normalizable with respect to energy outside the optimum ball size range. A liberation model which accounts for ball size changes would require some type of functional form to predict particle breakage.

The changes in energy specific breakage rates related to changes in ball size are much more prominent for material that is rich in sphalerite. In fact, as the amount of sphalerite content increases the spread in the energy specific breakage rates also increases.

The effect of interstitial filling on the specific breakage rates of various particle classes is shown on Figure 4.7. From this figure it can be seen that free dolomite tends to normalize well with respect to energy. As the amount of sphalerite content increases, the breakage rates become non-normalizable. Once again, it seems that the differences in breakage kinetics within the mill for particles containing sphalerite are more prominant. The hindering of breakage rates for composite materials and sphalerite is not a function of the increased power draw due to more material, but a change in the breakage mechanisms. It should also be noted that overcharging the mill to 150% interstitial filling caused a significant hindrance of composite particle breakage, more so than with liberated

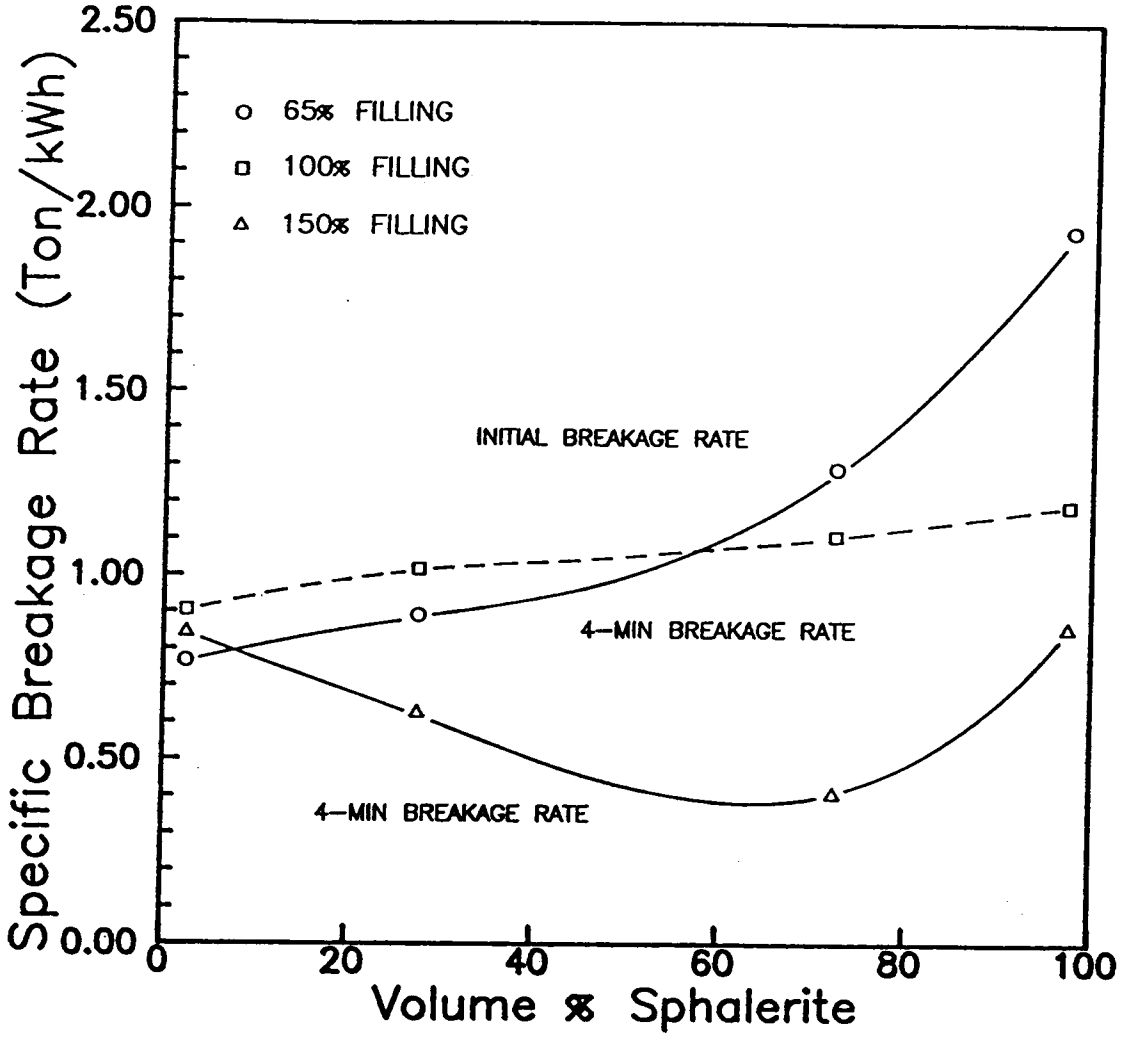

Figure 4.7 Energy normalized breakage rates versus percent sphalerite for different interstitial fillings with 10x14 mesh feed.

material. This would tend to confirm that composite particles are more susceptible to overcharging and the associated cushioning effect. The introduction of mill filling as a variable in a general liberation model would require a functional form for material containing sphalerite. On the other hand, dolomite would require a simple energy relationship in the prediction of its breakage characteristics.

Figure 4.8 illustrates the energy specific breakage rates for a dry and 70% solids grinding environment on 14 x 20 mesh feed. From the data collected it is apparent that the changes in breakage rates are non normalizable with respect to energy. The inclusion of this parameter into a generic liberation model would certainly require a functional relationship to describe particle breakage.

4.3 Comparison of Experimental Results to Previous Work:

It should be noted that direct comparisons to previous work are not possible since these studies have been based on homogeneous material. It is possible however, to compare trends that have been observed with changes in mill operating parameters and there effect on breakage rates. For the convenience of comparison, the collected data has been plotted with the independent variable being the mill parameter, and the dependent variable being the breakage

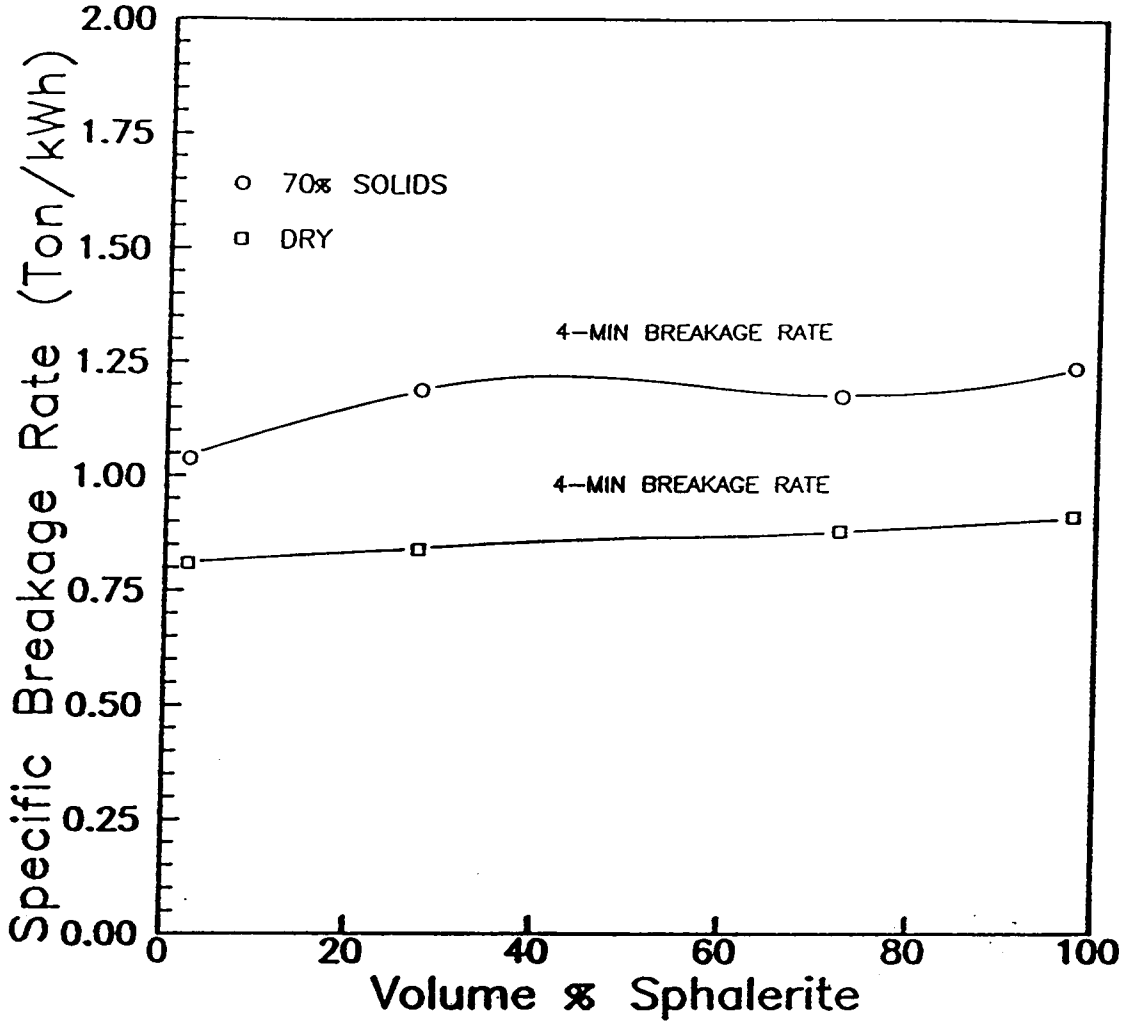

Figure 4.8 Energy normalized breakage rates versus percent sphalerite for dry and 70 percent solids grinding environments with 14x20 mesh feed.

rate achieved. This has been done for the ball size and mill filling experiments with each of the compositions of particles as can be seen on Figures 4.9 and 4.10.

In the case of mill speed, Herbst and Fuerstenau (1972) found a mill speed of 75% critical speed provided the optimum breakage rate of 7 x 9 mesh dolomite. This was accomplished by varying the mill speed from 30 to 90% critical speed. From the two mill speeds tested in this investigation, 85% critical speed was found to provide substantially better breakage rates than that of 40% critical speed for all the particle classes. However, the enhancement of breakage rates due to and increase in mill speed was much more pronounced for particles rich in sphalerite.

Analyzing the energy specific breakage rates obtained for the mill speed parameter, it was found that breakage rates of the liberated components were generally normalizable with respect to energy. Similar results were presented by Herbst and Fuerstenau (1973) for the grinding of pure dolomite.

Figure 4.9 illustrates breakage rates as a function of ball size. In general it can be seen that an optimum ball size significantly increases the breakage rates for all the particle classes. Similar responses to ball size changes were observed by Gupta and Kapur (1974) and Gupta, Zouit and

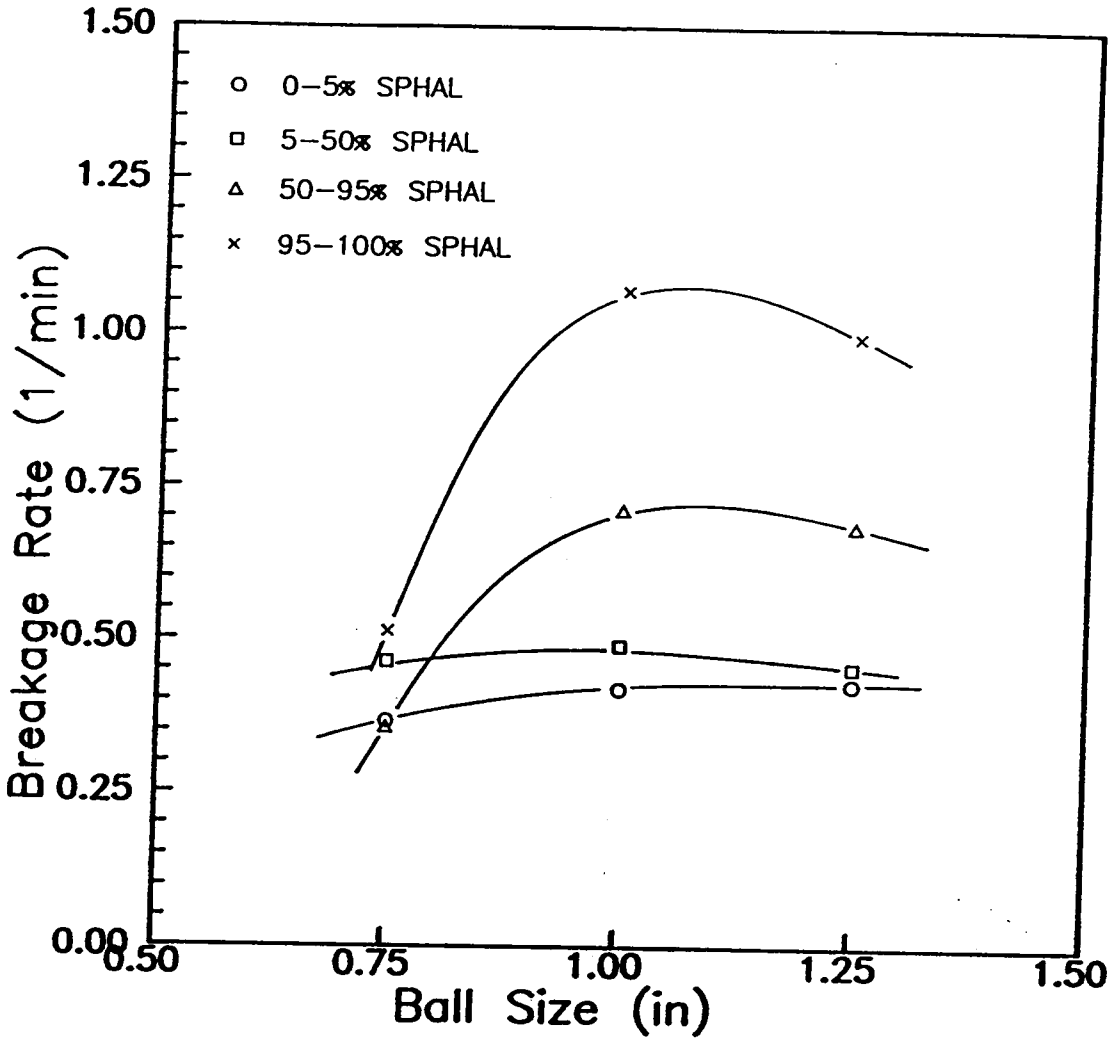

Figure 4.9 Breakage rate versus ball size for different sphalerite content material with 10x14 mesh material.

Hodouin (1984). Both investigations as well as others have shown that the use of a ball size other than the optimum results in significant drops in breakage rate values. It should be noted that the effect of ball size on breakage rates increases with the amount of sphalerite present. In the case of the 0 to 5% sphalerite class, little change was noted as a result of ball size. Dolomite's low sensitivity to ball size changes would tend to explain the lack of a clear maximum value for this particular class.

It is also interesting to note that the optimum ball size to particle size ratio was 18:1. This is comparable to the 20:1 ratio observed for stirred ball mill grinding of coal (Mankosa et al., 1986).

The effect of varying the percent interstitial filling on breakage rates correlated well with results obtained by Austin, Smaila, Brame, and Luckie, 1981 as well as other investigations. From a point of optimum interstitial filling, an increase in mill feed causes a decrease in breakage rate which is practically linear with respect to percent interstitial filling for all classes other than liberated sphalerite. The decay of breakage rates for liberated sphlaterite followed a more pronounced exponential type decay in breakage rates. Figure 4.10 shows these trends for each composition class.

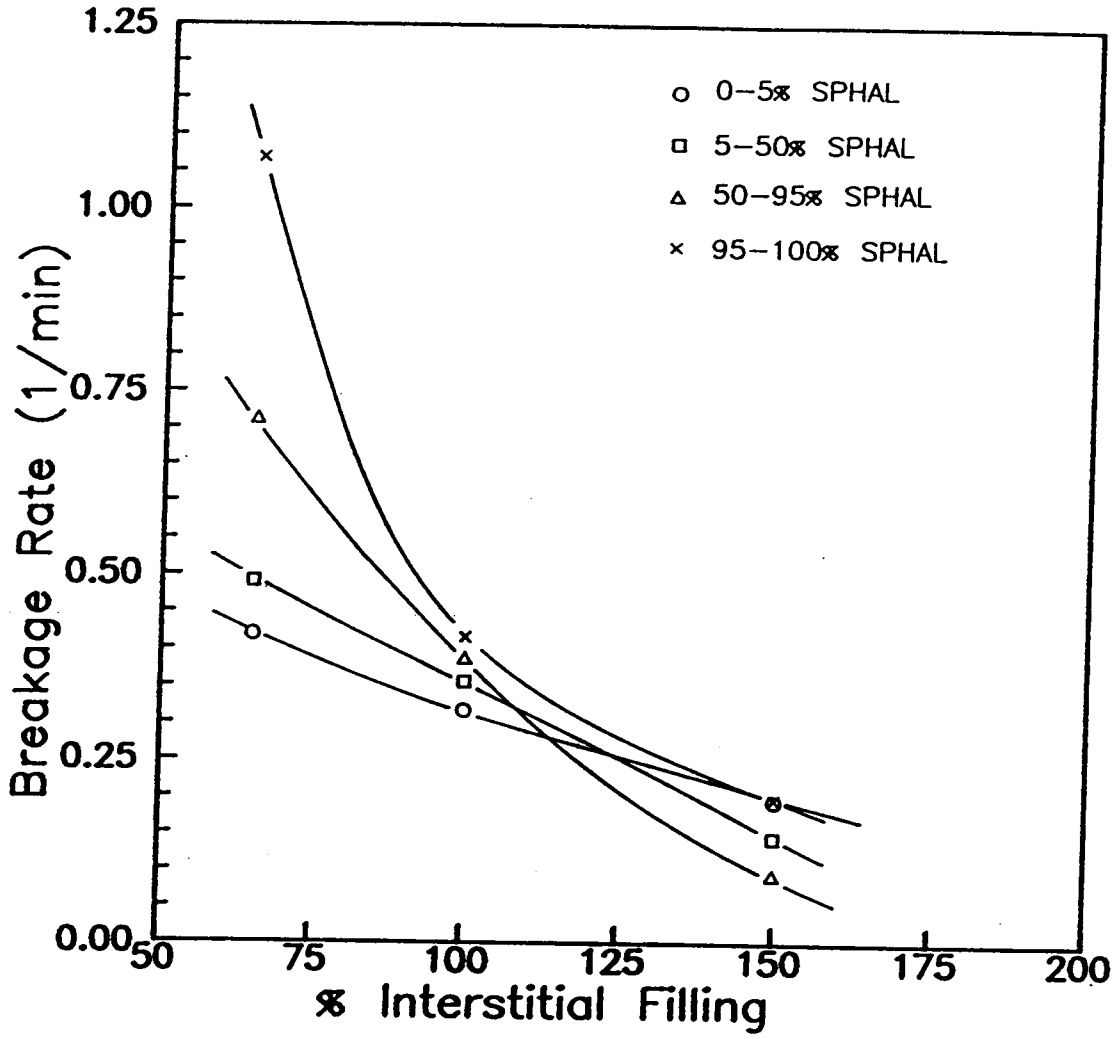

Figure 4.10 Breakage rate versus percent interstitial filling for different sphalerite content material with 10x14 mesh feed.

Since only one wet test was conducted at 70% solids, no plot has been generated. However, as noted by several investigators, wet grinding significantly enhances breakage rates as compared to dry grinding. This was found to be true with all the particle compositions.

CHAPTER V.

SUMMARY AND CONCLUSIONS

The major findings from the present investigation may be summarized as follows:

1. Changing mill speed greatly affected breakage rates of all the composition classes of 14x20 mesh material. The most effective mill speed for this investigation was that of 85% critical speed. Moving from an attrition breakage to an impact breakage environment shifts the optimum breakage rates for composite classes from 5-50% sphalerite to 50-95% sphalerite. In general, a change in mill speed is energy normalizable for liberated components, indicating that the changes observed are simply a function of energy input. Integration of mill speed into a liberation model would require a simple energy relation to quantify the expected breakage rates of liberated components and a functional relationship for composite classes.
2. In general, an optimum ball size of 1 inch greatly increased the breakage rates for 10x14 mesh

material. Changes in ball size affected the breakage rates directly as a function of sphalerite content. The higher the sphalerite content, the greater the influence of ball size. The non normalizability of the optimum ball size with respect to energy, indicates that a functional form will be required for the prediction of breakage rates. Plotting the energy specific breakage rate versus the percent sphalerite of each class of particles, provided similar curve shapes for ball sizes close to optimum. This could possibly lead to a simpler development of a general functional form to predict breakage rates with changing ball size within a narrow range of ball sizes.

3. Increasing the mill filling to overloaded conditions of 150% interstitial filling significantly hindered the breakage of composite material as well as that of sphalerite. Dolomite breakage rates were found to normalize with respect to energy while particles containing sphlaterite and free sphlaterite did not. This phenomenon is attributed to attrition being the dominant breakage mechanism for dolomite. The manner in which mill filling can be included into

a generic liberation model seems to be wholly dependent on the material itself. In the case of dolomite, a simple specific energy relation could be used to predict particle breakage under different mill fillings. However, the introduction material such as sphalerite would require a complex functional relationships. The irregular changes in breakage rates and the non normalizability of mill charge with respect to energy, would make this a very difficult parameter to use in the prediction of breakage rates. A complex functional form would have to be used to have this parameter included into a liberation model.

4. Wet grinding as compared to dry grinding provided increased breakage rates for all the composition classes. The parameter was non normalizable with respect to energy for all the composition classes. This finding indicates that a functional relation would be required for this parameter to be included in a generic liberal model.

5. In general, changes in mill operating parameters caused substantially small changes in the specific breakage rates of dolomite. This phenomenon could account for some of the discrepancies reported in

literature related to the energy normalizability of breakage rates with changes in mill operating parameters.

6. From the information gathered, it seems that the primary breakage mechanism for sphalerite is that of impact breakage. This is supported by experimental tests that provided enhanced impact breakage conditions. Furthermore, it seems that attrition seems to be the dominant breakage mechanism for dolomite since an enhancement of impact conditions yielded smaller changes in breakage rates as compared to particles containing sphalerite. This information could be useful in mill design with the objective of increasing the liberation of sphalerite. Improving the mill's impact qualities would enhance the breakage of composite material thereby bettering liberation.

CHAPTER VI.

SUGGESTIONS FOR FUTURE WORK

From the information that was gathered in this investigation, the following areas of study are recommended for future projects:

1. It would be of great value to expand the ranges of parameter changes to see if the trends observed hold in more extreme cases. Assuming they are consistent, a preliminary attempt should be made to create functional forms for the prediction of breakage rates with parameter changes. These predicted breakage rates should be compared with experimental values to see the limitations of the predictions and the operating ranges that would be appropriate.
2. An attempt should be made at quantifying the effect of a change in feed composition as a function of time, to simulate recirculating loads. This could be accomplished by adding pure dolomite, sphalerite, or composite material to the original feed and analyzing the resulting changes in breakage rates and distribution functions.

3. Multi-component ore should be used with similar experimental approaches to see if trends are inherent solely to this mineral system, or can be indicative of other systems as well.
4. Mill parameter effects on breakage distribution functions should be analyzed directly. The resulting values should be compared to parameter estimation techniques to simplify calculations.
5. Detailed studies should be conducted once liberation models which incorporate mill operating parameters have been developed.
6. A greater emphasis should be placed on wet grinding experimentation. This would give a more practical approach industrially speaking.
7. A mixture of ball sizes, and even a distribution of ball sizes should be used to simulate actual conditions within a ball mill. This once again would provide information which would have greater applicability to industry.
8. The addition of chemical additives has been known to help in the dynamics of grinding, especially at high pulp density values. It would be of interest to see how the incorporation of these chemicals would affect the breakage of both liberated and locked particles.

9. It would be of great interest to conduct batch flotation tests after grinding under set mill conditions at various times to quantify liberation (in place of traditional image analysis techniques). If the grade recovery curves were substantially different, this process could greatly minimize the time requirements in quantifying liberation. Grades and recoveries could be considered a measure of liberation, which in turn would yield industrial application.

REFERENCES

Andrews, S.R. G. and Mika, T.S. 1976 "Comminution of a Heterogeneous Material: Development of a Model for Liberation Phenomena," Proc. 11th Int. Miner Processing Congr., Cagliari, pp. 59-88.

Austin, L.G. and Bhatia, V., 1971. "Experimental Methods for GrindingStudies in Laboratory Mills," Powder Technology, V. 5, pp. 261.

Austin, L.G., Klimpel, R.R. and Luckie, P.T., 1976. Process Engineering of Size Reduction: Ball Milling, Published by SME-AIME, New York.

Austin, L.G., Shoji, K., Luckie, P.T., 1976. "The effect of Ball size on Mill Performance," Powder Technology, V. 14, pp. 71-79.

Austin, L.G., Smaila, F., Brame, K. and Luckie, P.T., 1982. "FurtherStudies of Ball and Powder Filling Effects in Ball Milling," PowderTechnology, V. 31, pp. 121-126.

Bagga, P.S. and Luckie, P.T., 1983. "A Monte Carlo Simulation of Liberation Phenomena," Proceedings of First Conference on Use of Computers in Coal Industry, Y.J. Wang and R.L. Sanford, Ed., AIME, New York, pp. 247-250.

Barbery, G., 1974. "Determination of Particle Size Distribution from Measurements on Sections," Powder Technology, V. 9, pp. 231-240.

Berube, M.A., Berube, Y. and LeHouillier, R., 1979. "A Comparison of Dry and Wet Grinding of a Quarzite in a Small Batch Mill," Powder Technolgy, V. 23, pp. 169-178.

Bloise, R., Gateau, G. and Broussund, A., 1984. "Determination of Mineral Liberation in Ore Dressing," Eighth International Symposium of Application Computers and Mathematics in Mineral Industries, London, pp. 427-439.

Choi, W.Z., 1986. "A Combined Size Reduction and Liberation Model of Grinding," PhD Thesis, Dept. of Mining and Minerals Engineering, Virginia Polytechnic Institute and State University, Blacksburg, Virginia.

Davy, P.J., 1984. "Probability Models for Liberation," Journal of Applied Probability, V. 21, pp. 160-169.

Delesse, A., 1848. "Procede Mechanique Pour Determiner la Composistion des Roches," Ann Mines, (iv) 13, pp.139.

Finlayson, R.M. and Hulbert, D.G., 1980. "The Simulation of the Behavior of Individual Minerals in a Closed Grinding Circuit," Proceeding, 3rd IFAC Symposium, Montreal, pp. 323-332.

Forssberg, E. and Zhai H., 1987. "Three Dimensional Behaviour of the Key Parameters Affecting Grinding in a Batch Ball Mill," Scandinavian Journal of Metallurgy, V. 15, pp. 53-56.

Fuerstenau, D.W. and Sullivan, D.A., 1962. "Analysis of the Comminution of Mixtures in Ball Mills," Canadian Journal of Chemical Engineers, V. 40, pp. 43-50.

Fuerstenau, D.W. and Sullivan, D.A., 1962. "Size Distributions and Energy Consumption in Wet and Dry Grinding," AIME Trans, V.220, pp. 379-402.

Gupta, V.K., Hodouin, D., Berube, M.A., and Everell, M.D., 1981. "The Estimation of Rate and Breakage Parameters From Batch Grinding Data for a Complex Pyritic Ore Using Back-Calculation Method," Powder Technology, V.28, pp. 97-106.

Gupta, V.K. and Kapur, P.C., 1974. "Empirical Correlations for the Effects of Particulate Mass and Ball Size of the Selection Parameters in the Discretized Batch Grinding Equation," Powder Technology, V.10, pp. 217-223.

Gupta, V.K, Zouit, H. and Hodouin, D., 1985. "The Effect of Ball and Mill Diameters on Grinding Rate Parameters in Dry Grinding Operation," Powder Technology, V.42, pp. 199-208.

Herbst, J.A. and Fuerstenau, D.W., 1968. "The Zero Order Production of Fine Sizes in Comminution and Its Implications in Simulation." Trans. SME AIME, V.241, pp. 538-548.

Herbst, J.A. and Fuerstenau, D.W., 1972. "Influence of Mill Speed and Ball Loading on the Parameters of the Batch GRinding Equation," Trans. SME AIME, V.252, pp. 169-176.

Herbst, J.A. and Fuerstenau, D.W., 1973. "Mathematical Simulation of Dry Ball Milling Using Specific Power Information," Trans. SME AIME, V.254, pp. 343-348.

Kelsall, D.F., Reid, K.J. and Restarick, C.J., 1968/1969. "Continuous Grinding in a Small Wet Ball Mill Part II. A Study of the Influence of Hold-Up Weight," Powder Technolgy, V.2 pp. 162-168.

Kuwahara, Y., 1971. "Experimental Study of Selection Function and Distribution Function," Journal of Chemical Engineering, Japan, V.4 No.4, pp. 359-363.

King, R.P., 1978. "Determination of Particle Size Distribution from Measurements on Sections," Powder Technology, V.21, pp.147-150.

King, R.P., 1979. "A Model for the Quantitative Estimation of Mineral Liberation by Grinding," International Journal of Mineral Processing, V.6, pp. 207-220.

King, R.P., 1982. "The Prediction of Mineral Liberation from Mineral Texture," XIV MPC, Toronto, Vlll 1.1-1.18.

Klimpel, R.R and Austin, L.G., 1983. "A Preliminary Model of Liberation from a Binary System," Powder Technology, V. 34, pp. 121-130.

Le Houillier, Van Neste, A. and Marchand, J.C., 1977. "influence of Charge on the Parameters of the Batch Grinding Equation and Its Implications in Simulation," Powder Technology, V.16, pp. 7-15.

Li, T.M., 1976. "The new Look at Asarco's Tennessee Mines," Mining Engineering V.27, pp. 37-41.

Lin, C.L., 1986. "Measurement and Prediction of Mineral Liberation During Grinding," Ph.D. Thesis, Dept. of Metallurgy and Metallurgical Engineering, Univ. of Utah, Salt Lake City, Utah.

Lin, C.L., Miller, J.D. and Herbst, J.A., 1987 "Solutions to the Transformation Equation for Volumetric Grade Distributions from Linear and/or Areal Grade Distributions," Powder Technology V.50, pp. 55-63.

Lo, Y.C. and Herbst, J.A., 1986. "Consideration of Ball Size Effects in the Population Balance Approach to Mill Scale-Up," in: Advances in Mineral Processing (P. Somasundaran, ed.), SME-AIME, Littleton, Colorado, pp. 33-47.

Lynch, A., Whiten, W. and Draper, N., 1967. "Developing the Optimum Performance of a Multi-Stage Grinding Circuit," Trans. IMM, V.76, pp. C169-C182.

Mankosa, M.J., Adel, G.T. and Yoon, R.H., 1986. "Effect of Media Size in Stirred Ball Mill Grinding of Coal," Powder Technology, Vol. 49, pp. 75-82.

Miller, J.D. and Lin C.L., 1988. "Treatment of Polished Section Data for Detailed Liberation Analyis," International Journal of Mineral Processing, V.22, pp. 1-18.

Tangsathitkulchai, C. and Austin, L.G., 1985. "The effect of Slurry Density on Breakage Parameters of Quartz, Coal and Copper Ore in Laboratory Ball Mill," Powder Technology, V.42, pp. 287-296.

Thompson, E., 1930. "Quantitative Microscope Analysis," Journal of Geology, V.27, pp. 276.

Underwood, E.E., 1970. Quantitative Stereology, Addison-Wesley, Reading, Mass.

Wiegel, R.L. and Li, K., 1967. "A Random Model for Mineral Liberation by Size Reduction," Trans. SME AIME, V.238, pp. 179-189.

Yang, D., Mempel, G. and Fuerstenau, D.W., 1967. "A Laboratory Mill for Batch Grinding Experimentation," Tran. SME AIME, V.238, pp. 273-275.

APPENDIX I

Image Analysis Data

TABLE I-1. Sphalerite Distributions in 14x20 mesh for various grinding times at 40% critical speed.

ZnS Content (Wt%)	Grinding, Time, minutes			
	0.00	1.00	2.00	4.00
0-5	72.86	72.90	75.25	77.38
5-50	6.36	5.44	4.90	4.45
50-95	2.97	3.19	2.75	2.46
95-100	17.81	18.47	17.10	15.71

TABLE I-2. Sphalerite distributions in 14x20 mesh for various grinding times at 85% critical speed

ZnS Content (Wt%)	Grinding, Time, minutes			
	0.00	1.00	2.00	4.00
0-5	72.86	75.29	77.34	79.40
5-50	6.36	6.35	5.45	5.37
50-95	2.97	2.32	1.67	1.91
95-100	17.81	16.03	15.54	13.32

TABLE I-3. Sphalerite distributions in 10x14 mesh for various grinding times with 3/4" ball size.

ZnS Content (Wt%)	Grinding, Time, minutes			
	0.00	1.00	2.00	4.00
0-5	82.79	81.11	85.72	87.93
5-50	7.08	7.69	5.50	5.51
50-95	2.33	2.60	2.53	1.87
95-100	7.79	8.60	6.25	4.70

TABLE I-4. Sphalerite distributions in 10x14 mesh for various grinding times with 1" ball size.

ZnS Content (Wt%)	Grinding, Time, minutes				
	0.00*	0.00**	1.00	2.00	4.00
0-5	70.23	82.79	79.34	83.97	88.27
5-50	6.10	7.08	7.45	5.44	5.60
50-95	4.53	2.33	3.34	3.44	1.65
95-100	19.13	7.79	9.87	7.15	4.47

* Feed used for 1 and 2 min grinding times.
**Feed used for 4 min grinding time

TABLE I-5. Sphalerite distributions in 10x14 mesh for various grinding times with 1 1/4" ball size.

ZnS Content (Wt%)	Grinding, Time, minutes				
	0.00*	0.00**	1.00	2.00	4.00
0-5	70.23	82.79	78.66	75.65	85.31
5-50	6.10	7.08	7.28	6.39	6.52
50-95	4.53	2.33	3.43	3.49	2.61
95-100	19.13	7.79	10.63	14.46	5.56

* Feed used for 1 and 2 minute grinding times.
**Feed used for 4 minute grinding time.

TABLE I-6. Sphalerite distributions in 10x14 mesh for various grinding times with 65% interstitial filling.

ZnS Content (Wt%)	Grinding, Time, minutes				
	0.00*	0.00**	1.00	2.00	4.00
0-5	70.23	82.79	79.34	83.97	88.27
5-50	6.10	7.08	7.74	5.44	5.61
50-95	4.53	2.33	3.34	3.44	1.65
95-100	19.13	7.79	9.87	7.15	4.47

* Feed used for 1 and 2 min grinding times.
**Feed used for 4 min grinding time

TABLE I-7. Sphalerite distributions in 10x14 mesh for various grinding times with 100% interstitial filling.

ZnS Content (Wt%)	Grinding, Time, minutes	
	0.00	4.00
0-5	82.33	86.22
5-50	5.70	5.11
50-95	2.88	2.27
95-100	9.09	6.39

TABLE I-8. Sphalerite distributions in 10x14 mesh for various grinding times with 150% interstitial filling.

ZnS Content (Wt%)	Grinding, Time, minutes	
	0.00	4.00
0-5	82.33	80.27
5-50	5.70	6.77
50-95	2.88	4.20
95-100	9.09	8.76

TABLE I-9. Sphalerite distributions in 14x20 mesh for various grinding times with 1" ball size (dry).

ZnS Content (Wt%)	Grinding, Time, minutes	
	0.00	4.00
0-5	75.39	78.52
5-50	5.02	4.94
50-95	3.35	2.96
95-100	16.24	13.58

TABLE I-10. Sphalerite distributions in 14x20 mesh for various grinding times with 1 in" balls and 70% solids.

ZnS Content (Wt%)	Grinding, Time, minutes			
	0.00	1.00	2.00	4.00
0-5	75.39	70.67	77.43	81.93
5-50	5.02	4.39	4.50	3.92
50-95	3.35	3.59	4.36	2.70
95-100	16.24	21.35	13.71	11.44

APPENDIX II

Percent Remaining Values for the Disappearance Plots

TABLE II-1. Percent remaining of original 14x20 feed for various grinding times at 40% critical speed.

ZnS Content (Wt%)	Grinding, Time, minutes			
	0.00	1.00	2.00	4.00
0-5	100.00	80.07	66.08	44.39
5-50	100.00	68.47	49.20	29.24
50-95	100.00	85.96	59.25	34.62
95-100	100.00	83.00	61.37	36.87

TABLE II-2. Percent remaining of original 14x20 feed for various grinding times at 85% critical speed.

ZnS Content (Wt%)	Grinding, Time, minutes			
	0.00	1.00	2.00	4.00
0-5	100.00	66.39	44.65	22.08
5-50	100.00	64.14	36.05	17.11
50-95	100.00	50.18	23.65	13.05
95-100	100.00	57.82	36.70	15.15

TABLE II-3. Percent remaining of original 10x14 feed for various grinding times with 3/4" ball size.

ZnS Content (Wt%)	Grinding, Time, minutes			
	0.00	1.00	2.00	4.00
0-5	100.00	65.11	46.71	22.62
5-50	100.00	72.21	35.07	16.56
50-95	100.00	74.19	48.94	17.07
95-100	100.00	73.34	36.18	12.85

TABLE II-4. Percent remaining of origninal 10x14 feed for various grinding times with 1" ball size.

ZnS Content (Wt%)	Grinding, Time, minutes			
	0.00	1.00	2.00	4.00
0-5	100.00	75.19	50.53	18.85
5-50	100.00	84.45	37.68	14.01
50-95	100.00	49.02	32.06	12.52
95-100	100.00	34.33	15.78	10.15

TABLE II-5. Percentremaining of original 10x14 feed for various grinding times with 1 1/4" ball size.

ZnS Content (Wt%)	Grinding, Time, minutes			
	0.00	1.00	2.00	4.00
0-5	100.00	74.23	40.34	17.98
5-50	100.00	79.30	39.23	16.08
50-95	100.00	50.26	28.82	19.54
95-100	100.00	36.92	28.30	12.45

TABLE II-6. Percent remaining of original 10x14 feed for various grinding times at 65% interstitial filling.

ZnS Content (Wt%)	Grinding, Time, minutes			
	0.00	1.00	2.00	4.00
0-5	100.00	75.19	50.53	18.85
5-50	100.00	84.45	37.68	14.01
50-95	100.00	49.02	32.06	12.52
95-100	100.00	34.33	15.78	10.15

TABLE II-7. Percent remaining of original 10x14 feed for various grinding times with 100% interstitial filling.

ZnS Content (Wt%)	Grinding, Time, minutes	
	0.00	4.00
0-5	100.00	28.09
5-50	100.00	24.06
50-95	100.00	21.16
95-100	100.00	18.85

TABLE II-8. Percent remaining of original 10x14 feed for various grinding times with 150% interstitial filling.

ZnS Content (Wt%)	Grinding, Time, minutes	
	0.00	4.00
0-5	100.00	45.78
5-50	100.00	55.77
50-95	100.00	68.47
95-100	100.00	45.25

TABLE 11-9 Percent remaining of original 14x20 feed for various grinding times with 1" balls (dry).

ZnS Content (Wt%)	Grinding, Time, minutes 0.00	4.00
0-5	100.00	16.68
5-50	100.00	15.77
50-95	100.00	14.14
95-100	100.00	13.40

TABLE II-10. Percent remaining of original 14x20 feed for various grinding times with 1" balls and 70% solids.

ZnS Content (Wt%)	Grinding, Time, minutes 0.00	1.00	2.00	4.00
0-5	100.00	55.21	35.01	9.95
5-50	100.00	51.51	30.55	7.15
50-95	100.00	63.12	44.36	7.37
95-100	100.00	77.43	28.78	6.45

APPENDIX III

Disappearance Plots

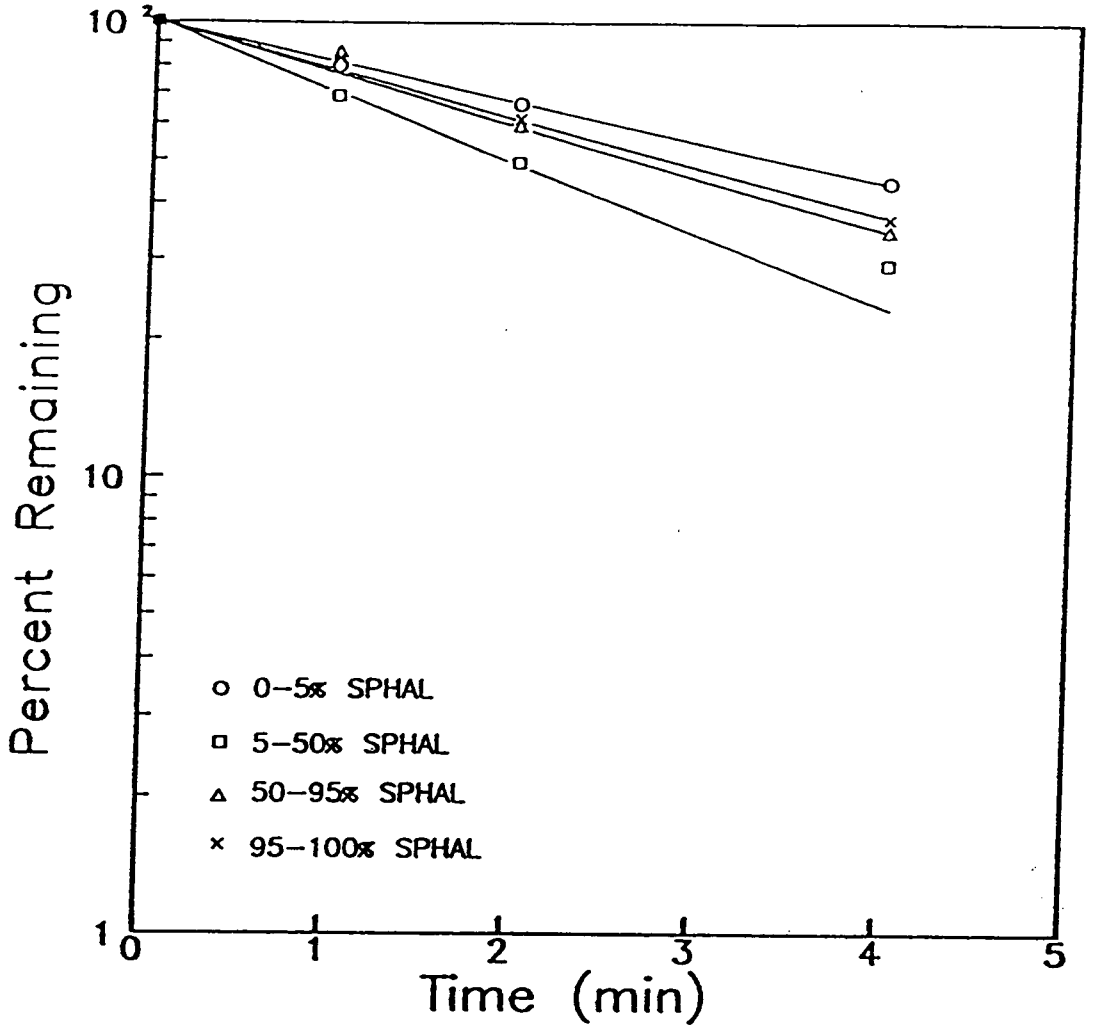

Figure III-1 Disappearance plot for a 14x20 mesh feed at 40% critical speed.

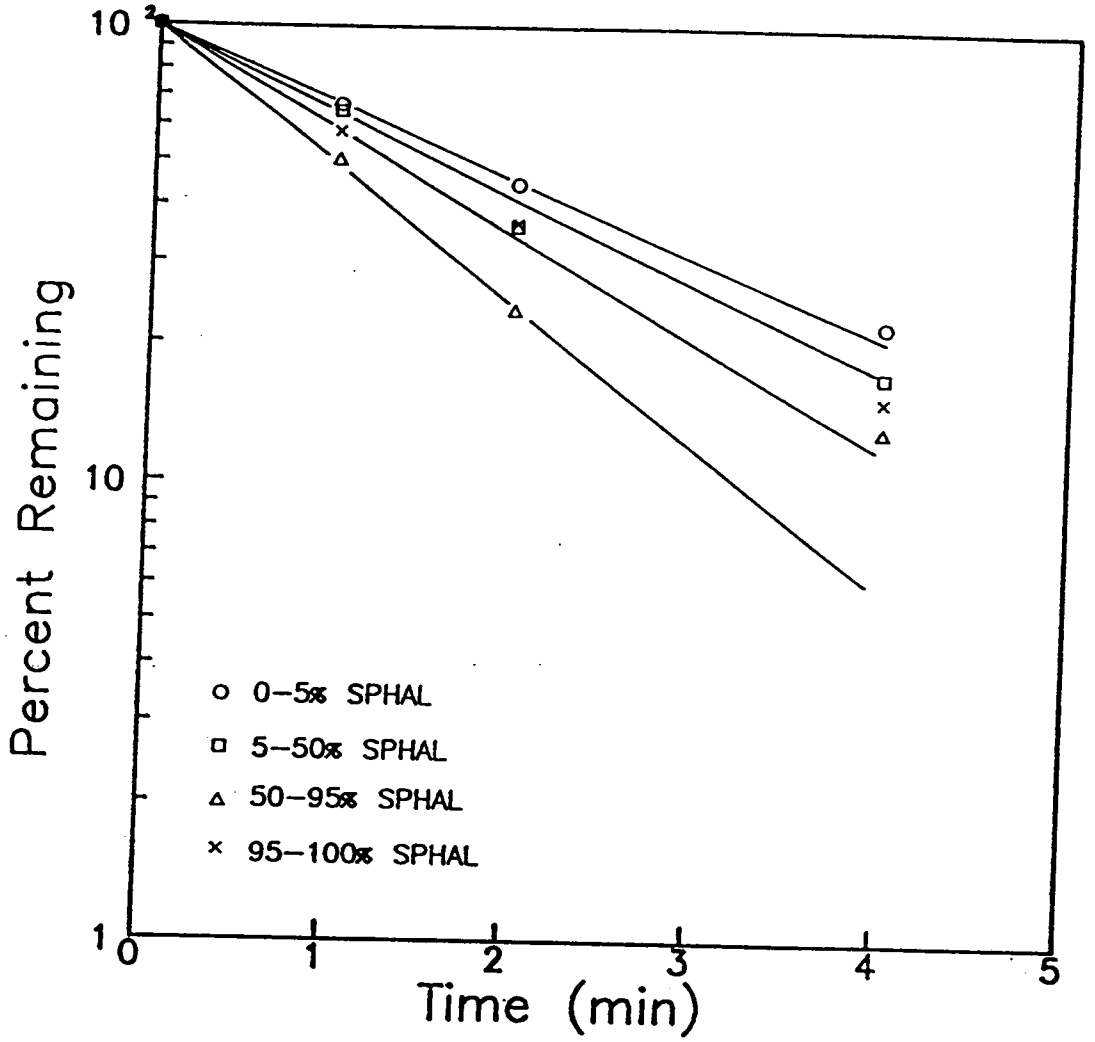

Figure III-2 Disappearance plot for a 14x20 mesh feed at 85% critical speed.

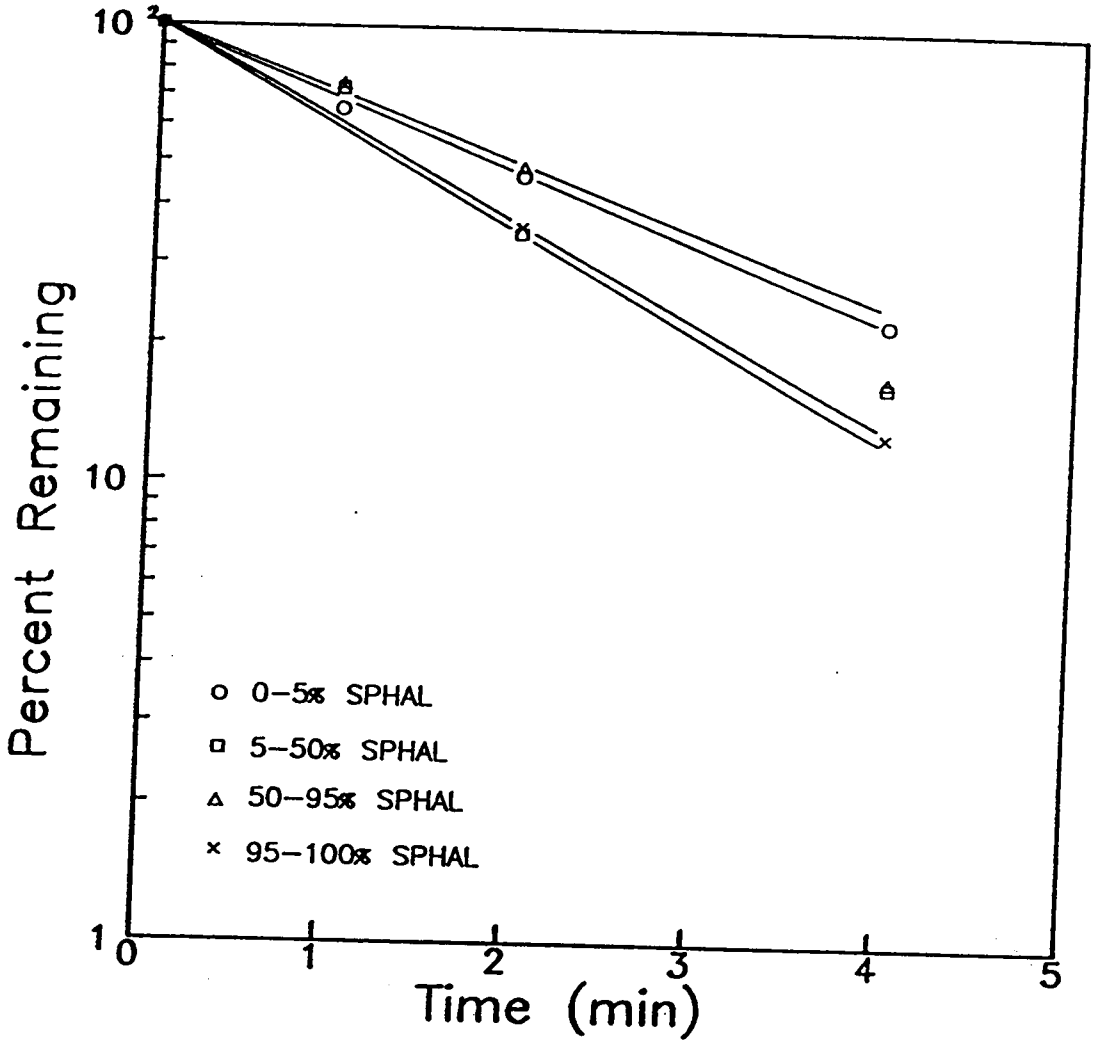

Figure III-3 Disappearance plot for a 10x14 mesh feed with a 3/4" ball size.

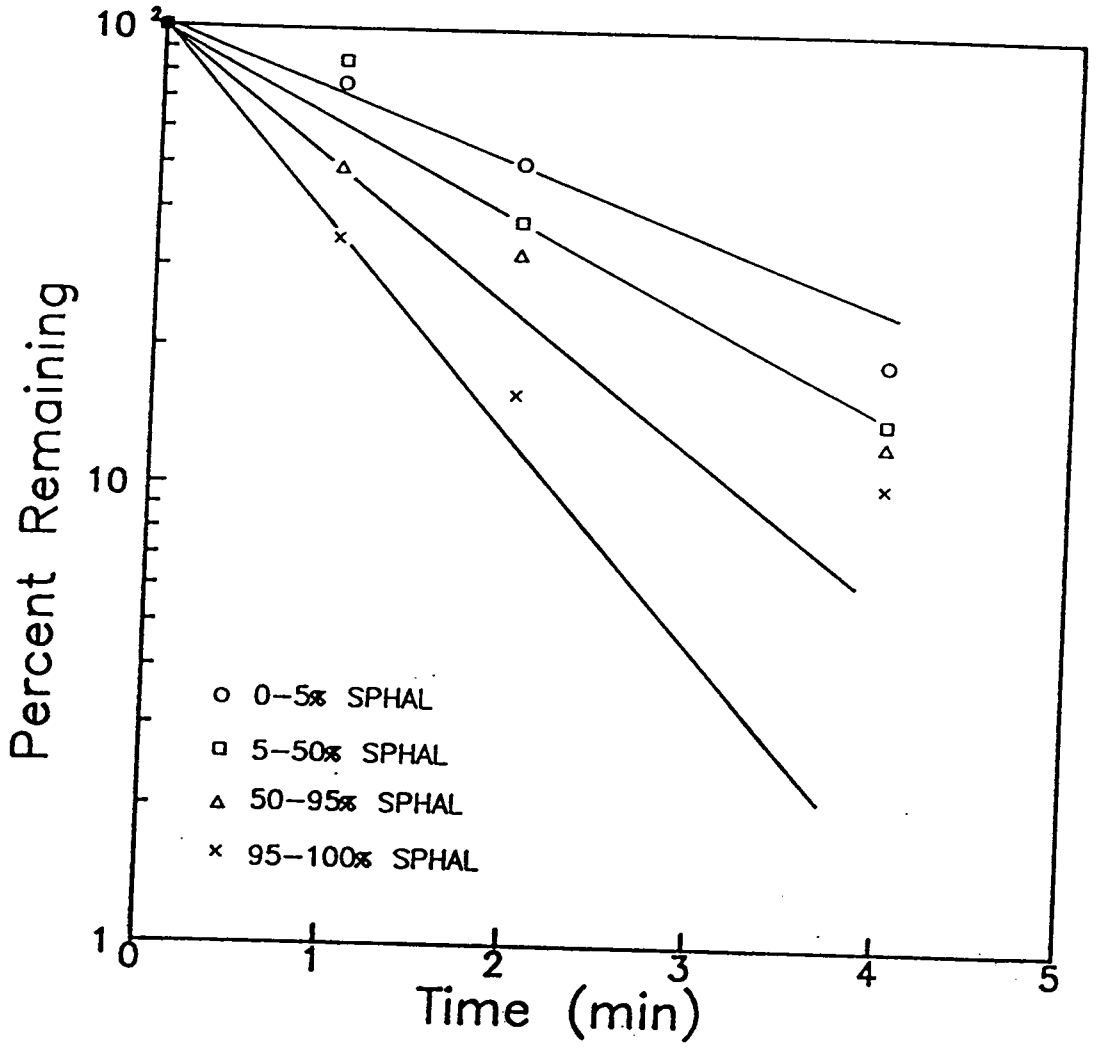

Figure III- 4 Disappearance plot for a 10x14 mesh feed with a 1" ball size.

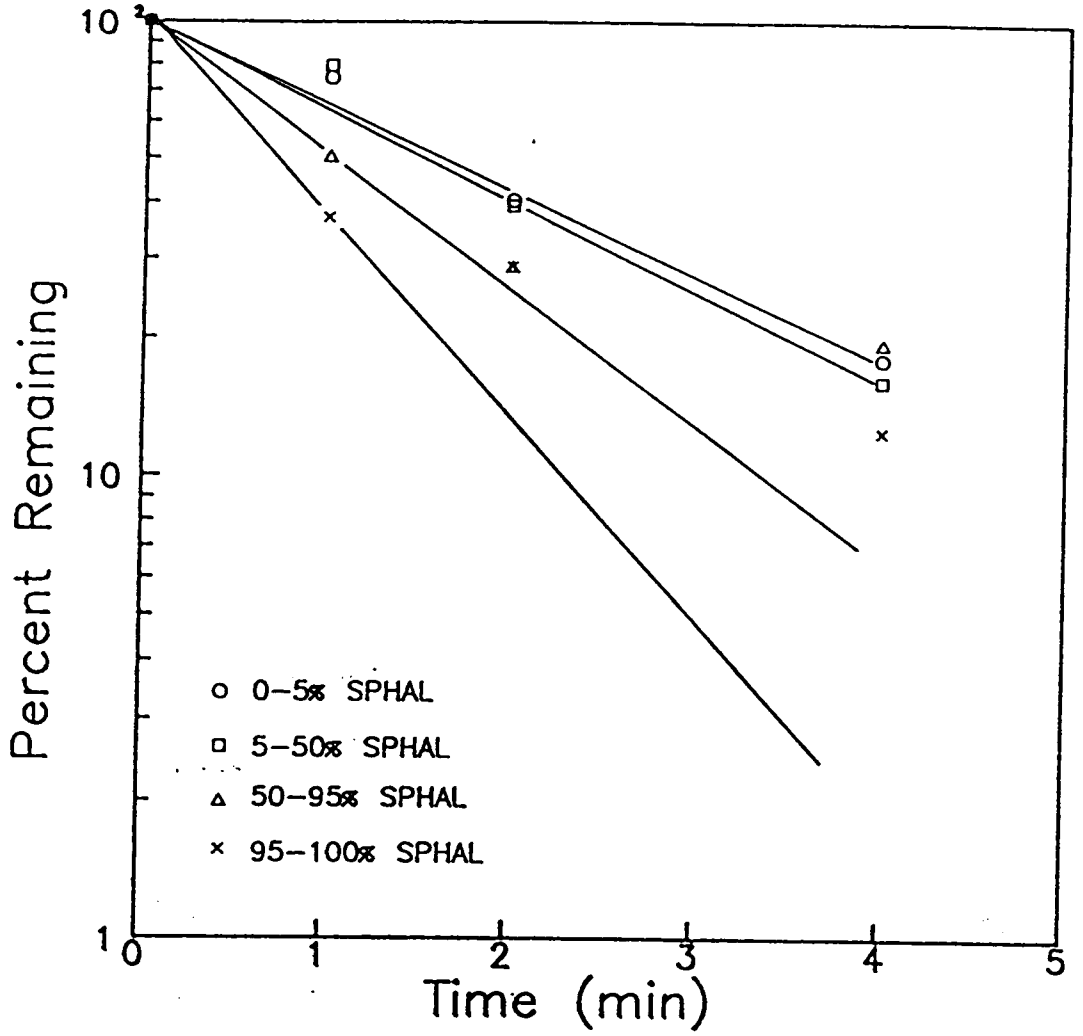

Figure III-5 Disappearance plot for a 10x14 mesh feed with a 1 1/4" ball size.

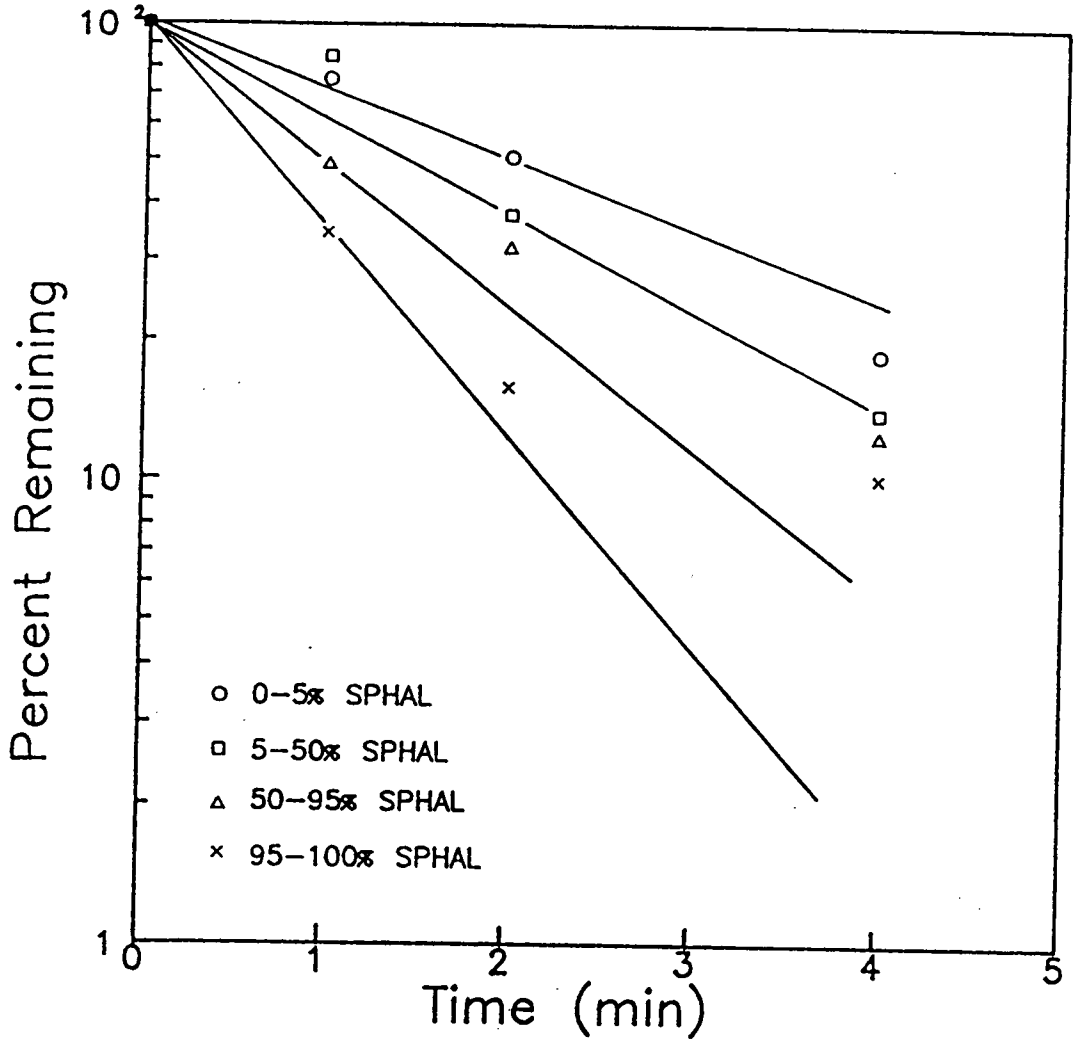

Figure III-6 Disappearance plot for a 10x14 mesh feed with a 65% interstitial filling.

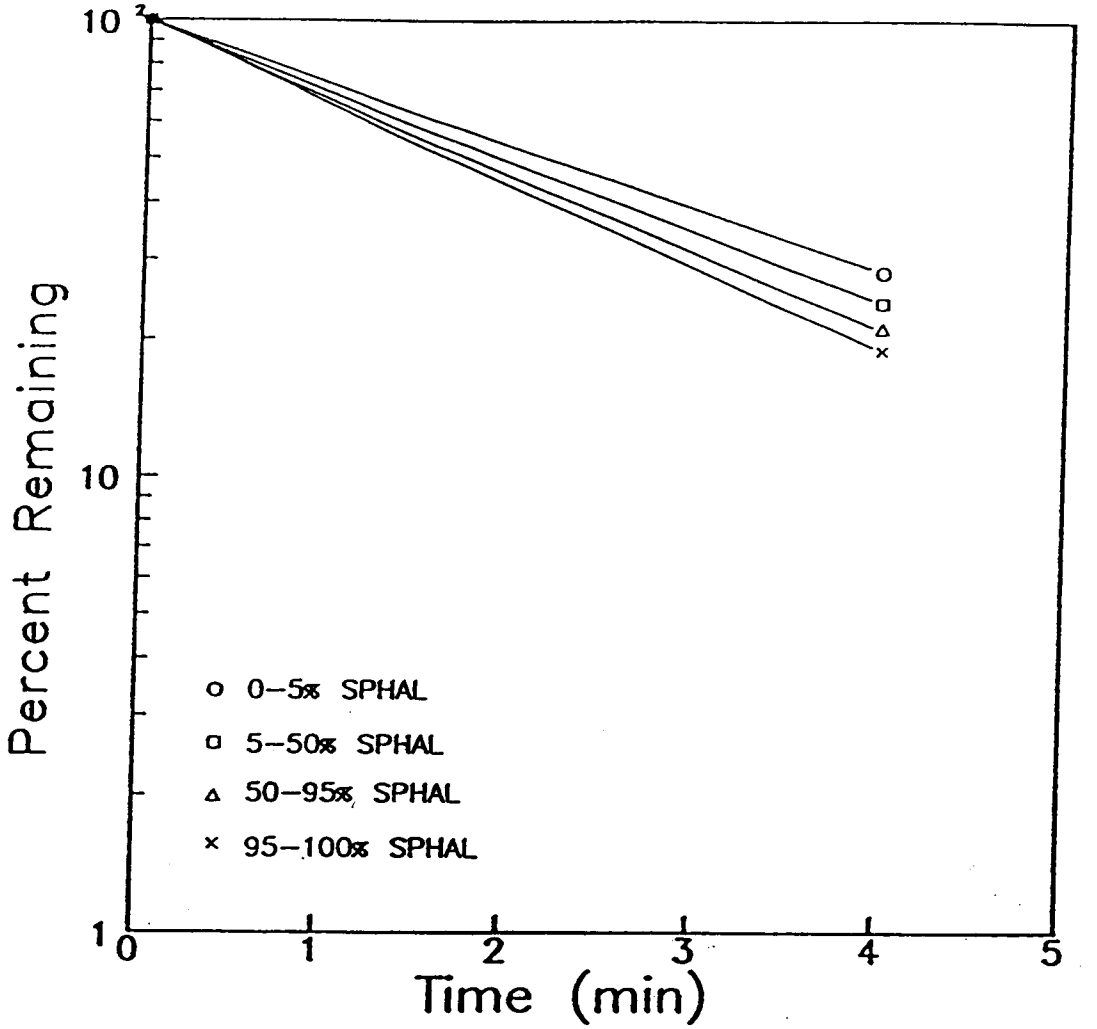

Figure III-7 Disappearance plot for a 10x14 mesh feed with a 65% interstitial filling.

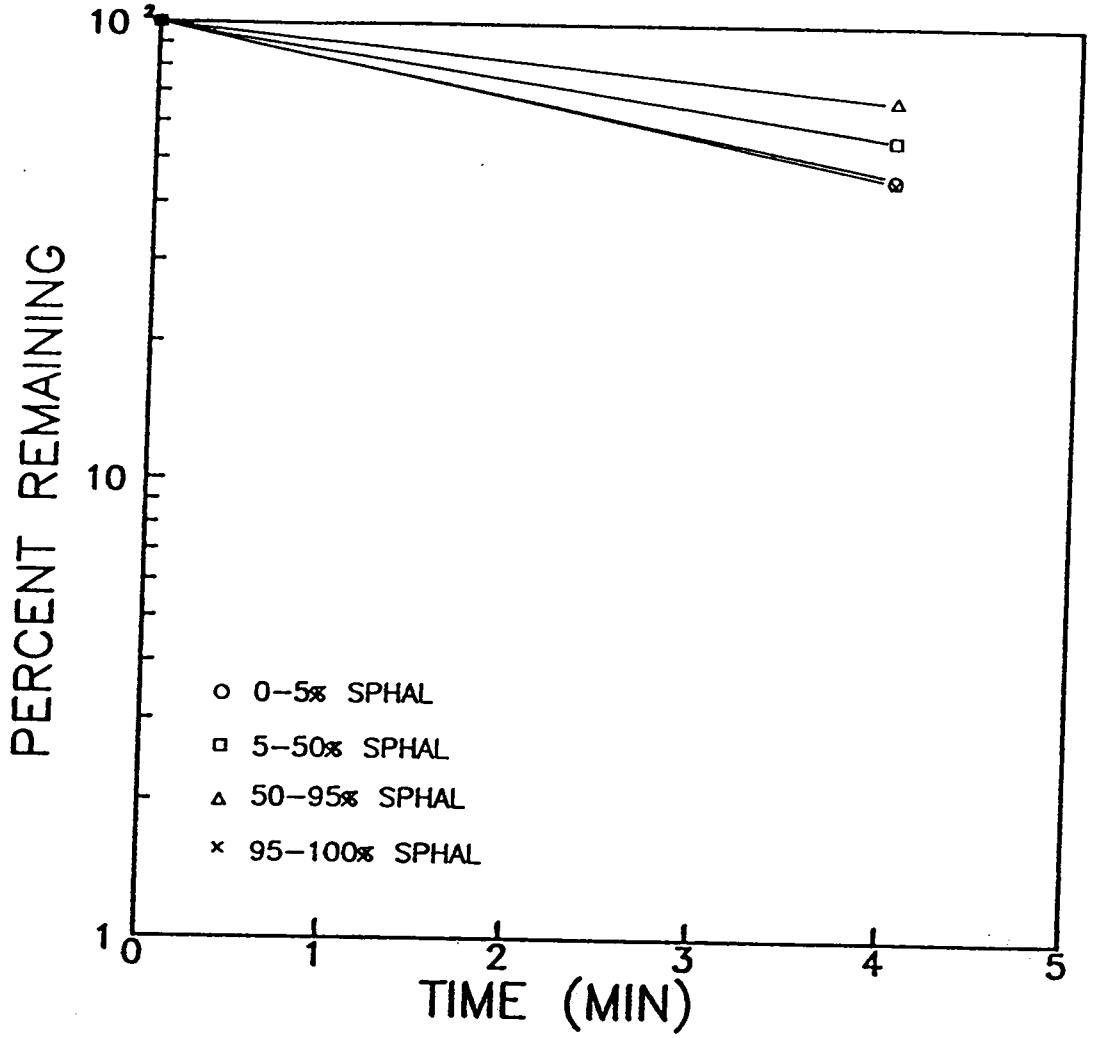

Figure III-8 Disappearance plot for a 10x14 mesh feed with a 150% interstitial filling.

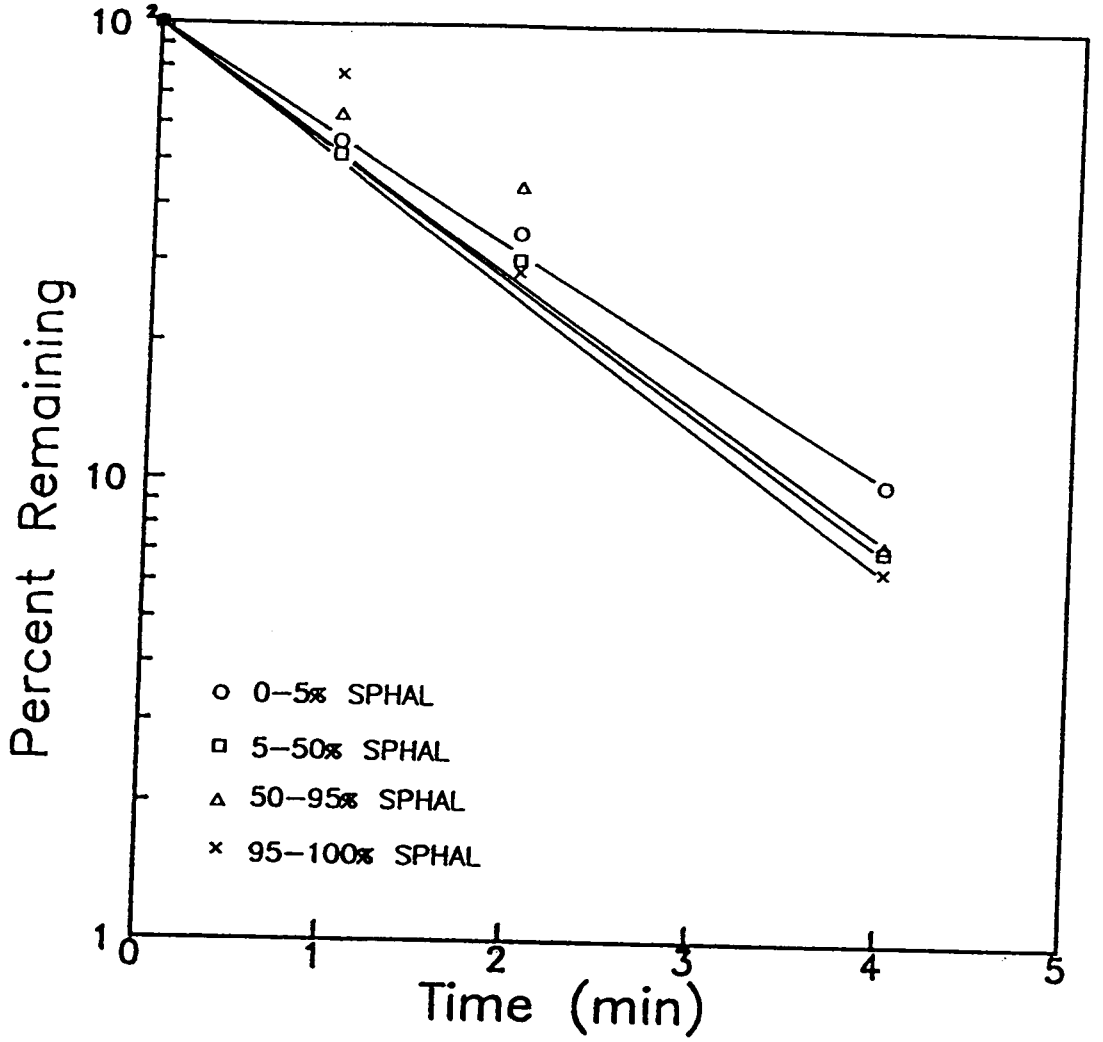

Figure III- 9 Disappearance plot for a 14x20 mesh feed with a 70% solids grinding environment.

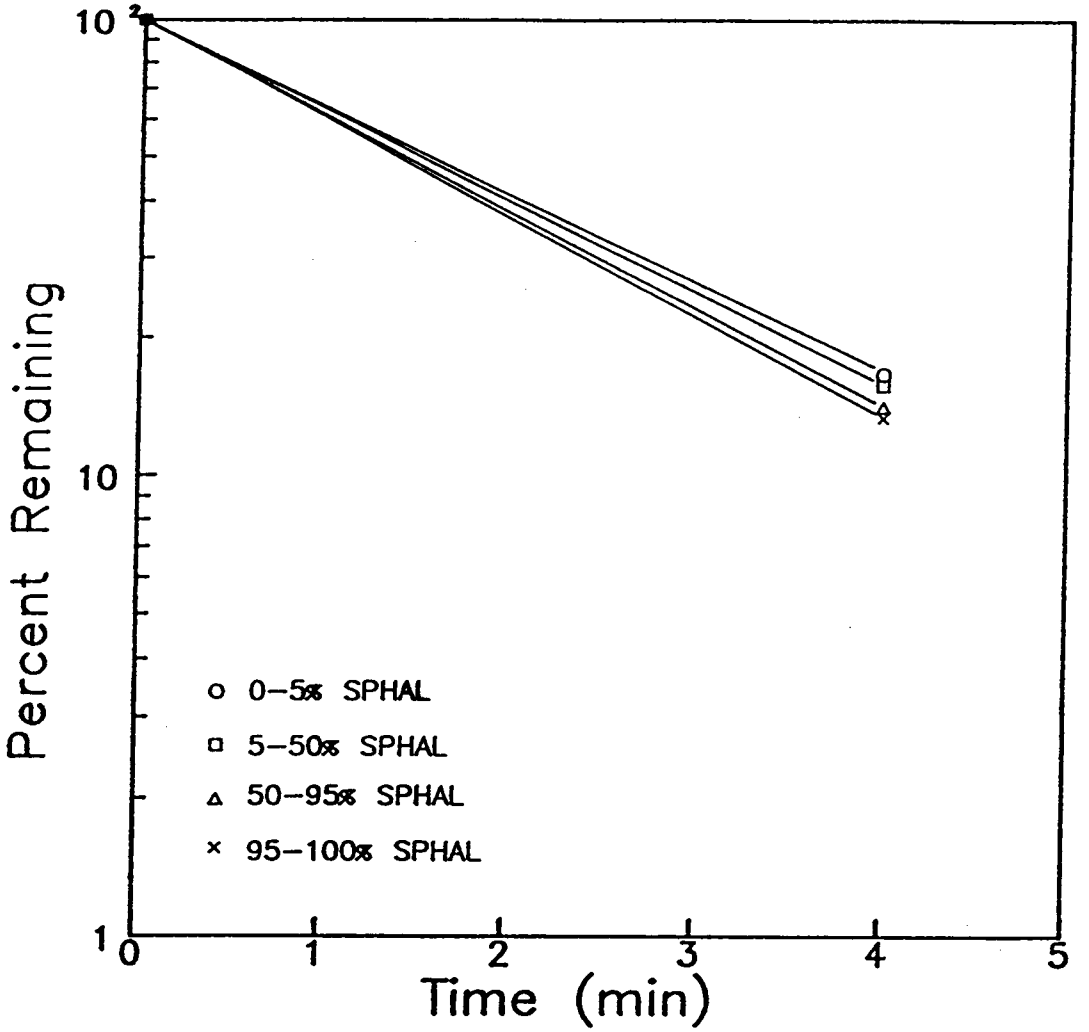

Figure III-10 Disappearance plot for a 14x20 mesh feed with a 100% solids grinding environment.

APPENDIX IV

Breakage and Energy Specific Breakage Rates

TABLE IV-1. Breakage and Specific Breakage Rates for RPM parameter in terms of percent critical speed.

ZnS Content (Wt%)	Breakage Rate (1/min)		Specific Breakage Rate (Tons/Kwhr)	
	40	85	40	85
0-5	.202	.403	.651	.738
5-50	.355	.441	1.145	.815
50-95	.265	.721	.857	1.319
95-100	.249	.548	.806	1.002

TABLE IV-2. Breakage and Specific Breakage Rates for ball size parameter in terms of ball size in inches.

ZnS Content (Wt%)	Breakage Rate (1/min)			Specific Breakage Rate (Tons/Kwhr)		
	3/4	1	1 1/4	3/4	1	1 1/4
0-5	.372	.424	.429	.676	.767	.819
5-50	.464	.491	.457	.845	.889	.873
50-95	.357	.713	.688	.650	1.290	1.314
95-100	.513	1.068	.996	.933	1.934	1.903

TABLE IV-3. Breakage and Specific Breakage Rates for mill charge parameter in terms of percent interstitial filling.

ZnS Content (Wt%)	Breakage Rate (1.min.)			Specific Breakage Rate (Tons/Kwhr)		
	65	100	150	65	100	150
0-5	.424	.317	.195	.767	.905	.848
5-50	.491	.356	.145	.889	1.015	.629
50-95	.713	.388	.095	1.290	1.107	.411
95-100	1.069	.417	.198	1.934	1.189	.860

TABLE IV-4. Breakage and Specific Breakage Rates for wet grinding parameter in terms of percent solids.

ZnS Content (Wt%)	Breakage Rate (1/min)		Specific Breakage Rate (Tons/Kwhr)	
	100	70*	100	70*
0-5	.448	.577	.810	1.039
5-50	.462	.660	.836	1.187
50-95	.489	.652	.885	1.173
95-100	.502	.686	.909	1.234

* Four minute grind values used for calculations.

APPENDIX V

Chemical Assay Procedure

ASSAY PROCEDURE: Samples of narrowly sized material were split into representative fractions of approximately 10 grams. A mechanical mortor and pestle was used for a period of 15 minutes to pulverize the specimens. Once pulverized, .5 grams were put into a 500 ml beaker. Twenty ml of concentrated hydrochloric acid was then added to the beaker, and allowed to digest the sample for approximately 10 minutes while heating the solution. Ten ml of concentrated nitric acid was then added to the beaker and digestion continued for 10 more minutes. The beaker was then allowed to cool and the solution was transferred to a 500 ml volumetric flask and made up to volume with distilled water.

The solution was then filtered through a Whatman #1 filter paper into a clean, dry 100 ml beaker and atomized through a Spectraspan IV Plasma Emission Spectrometer. The wave length used to detect zinc was 206.2 nm. Standards for calibration were made from a 1000 mg/l Fisher Scientific stock solution.

The vita has been removed from the scanned document